From Heatwaves to Cold Spells: How Extreme Temperature Events Shape Inflation in Germany

Michel Grimm University of Bremen *

Torben Klarl University of Bremen ‡

August 22, 2025

Preliminary Version. Please do not cite. Comments are welcomed!

Abstract

In this paper, we develop a novel methodology to identify temperature surprise shocks for hot and cold extreme weather events using granular ground station- and satellite-based weather data for Germany. We focus on food and energy prices, which are key drivers of inflation in Germany and, at the same time, are themselves strongly affected by climate-related shocks. A positive heat shock of one standard deviation increases food prices by up to 0.39% in summer, while the same type of shock in winter decreases energy prices by 0.88%. Moreover, our results indicate that food prices are driven primarily by supply-side factors, as the interaction of a heat shock with a drought variable amplifies the effect through its impact on agricultural production, whereas energy prices respond mainly to demand-side factors, such as changes in heating and cooling needs. Using our identified weather shocks, we estimate the causal effects of extreme temperatures on these two components and trace their pass-through to headline inflation. These results are robust when accounting for nonlinearities arising from seasonality and shock magnitude, the role of transmission channels such as renewable energy production, droughts, and different learning periods in which agents form expectations from past weather shocks.

Keywords: weather shock construction, granular weather data, energy prices, food prices, temperature shocks, business cycle, climate change

JEL: C32, E32, E52, Q54

*Faculty of Business Studies and Economics, Max-von-Laue-Straße 1, D-28359 Bremen, e-mail: E-Mail: michel.grimm@uni-bremen.de, Tel:+49 (0)421 218-66563

†Faculty of Business Studies and Economics, Max-von-Laue-Straße 1, D-28359 Bremen, e-mail: tklarl@uni-bremen.de, Tel.: +49 (0)421 218-66562

‡We thank Aaron Mehrotra, Robert Lehmann, Robert Czudaj, Valeriya Dinger, Stefan Eichler, Giang Nghiem, Erkan Gören, Gerrit Lohmann, and Martin Bodenstein; the participants at the ifo Dresden Workshop on Macroeconomics & International Finance; seminar participants at the EEA 2025 in Bordeaux, at Oldenburg, and at the 7^{th} Bundesbank Workshop for Young Scientists on Applied Economics in Hannover.

1 Introduction

This study develops a novel weather-shock identification strategy to examine how extreme cold and heat events affect inflation in Germany. Controlling for several confounding factors such as droughts, growing seasons, the growing importance of renewable energy sources and nonlinear interactions with precipitation, we find that weather shocks influence prices mainly through two channels: heightened energy demand and disruptions to food supply. Germany's particular energy mix[1] and agricultural structure make it especially sensitive to these channels, amplifying the inflationary effects of climate extremes. In particular, our results demonstrate that climate change is not only driving more frequent summer heatwaves, but is also intensifying a broad range of extreme weather conditions, including cold spells—a phenomenon well documented in the natural sciences but surprisingly underexplored in the economics literature (see Zohner et al. (2020) and references therein).

We contend that there are three main reasons for focusing on a single-country study. First, from a climate research perspective, Germany is an intrinsically interesting case: located in a climatic transition zone where maritime and continental influences converge, it is particularly sensitive to changes in the jet stream. Climate change induced shifts in the subpolar jet stream—projected to move poleward and become more sinuous—lead to more stagnant and extreme weather patterns[2]. Combined with high socio-economic and infrastructural exposure, these dynamics amplify the impacts of climate change, making them more pronounced than in European countries with more uniformly maritime or continental climates. Moreover, according to the latest Climate Risk Index, Germany ranks among the 50 coun-

[1] In 2023, Germany had the highest share of solar and wind in electricity production among European countries (39.88%), while the share of all renewable energy sources exceeded 50%, according to data from the International Energy Agency.

[2] Among others, Coumou et al. (2018) emphasizes that under anthropogenic climate change, the subpolar jet stream is projected to shift poleward and become more sinuous. These changes result in more persistent anomalies and extreme weather events—such as heatwaves, droughts, floods, and wildfires—in the mid-latitudes.

tries worldwide most affected by extreme weather events between 1993 and 2022[3]. Second, cross-country studies face the challenge that countries occupy different climatic zones, which may themselves shift over time due to climate change. This heterogeneity can introduce an omitted-variable bias in multi-country analyses that is difficult to address, given the complex atmospheric dynamical processes that characterize different zones. For example, Rousi et al. (2018) show that so-called double jet streams are a key driver of heatwaves in northern Europe, whereas persistent heatwaves in the Mediterranean and Eastern Europe are more likely sustained by land–atmosphere feedbacks linked to dry soil conditions. Thus, from an econometric point of view, we rather reconstruct the historical exposure of the population to climatic conditions and estimate the effects of temporal variation using standard econometric techniques, following Hsiang et al. (2013). Third, behavioral responses to climate shocks also vary by climatic history. In countries such as Italy or Spain, where heatwaves have historically been more frequent, people are less surprised by future climate shocks and therefore respond (economically) differently compared to those in Germany, where heatwaves are a relatively recent phenomenon.

In Germany, the average temperature rose by 16.65 percent between the 1970s and the 2010s. As shown in Figure 1, this trend masks considerable regional variation: areas in the far south experienced markedly larger increases, while other regions warmed less.[4] In contrast, our identified temperature shocks (details on identification follow) display a different spatial pattern, with northern Germany experiencing, on average, more frequent and more intense hot and cold extremes, amplifying the need of identifying a clean temperature shock instead of relying on level values.

Prices are of particular interest because they capture both direct supply-side effects and

[3]See https://www.germanwatch.org/de/cri.

[4]For clarity, the top 1 percent of regions in terms of temperature increase are excluded from the map, as they represent extreme outliers relative to the national average.

Figure 1: Growth rates of regional temperatures (1970s–2010s) alongside heat and cold temperature shocks as identified in this paper.

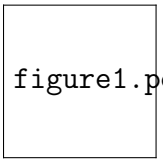

indirect demand-side or expectation-driven responses to weather shocks (Hsiang 2016). In recent years, monetary authorities, including the European Central Bank, are increasingly attentive to climate change, particularly regarding their implications for inflation monitoring and forecasting (ECB 2024; Drudi et al. 2021). Integrating climate change into monetary policy frameworks requires a clear understanding of the channels through which global warming influences prices. While the macroeconomic effects on output are relatively well documented, the relationship between temperature and prices—especially in advanced economies such as Germany—has received far less attention.

In this paper, we address four questions: 1) How do the reactions of individual price components to temperature shocks differ, and in what ways do these responses collectively influence the trajectory of overall inflation? 2) Are there differences between hot and cold extremes?[5] 3) Do prices respond linearly or are there nonlinear influences like calendar seasons or the size of the shock? 4) Does the transmission to renewable energy sources shift our results in a particular way?

To answer these questions, we introduce and employ a temperature shock identification strategy for Germany inspired by Natoli (2023), which departs from the standard anomaly-based measures used in most of the literature. This method accounts for both tails of the temperature distribution, enabling us to capture hot and cold extremes. It also incorporates agents' expectations and learning, ensuring that shocks represent unanticipated events. Using these shocks, we estimate their dynamic causal effects on prices via the local projection

[5]As highlighted before, climate change is increasing the frequency and intensity of extreme weather events, explicitly also cold extremes.

method of Jordà (2005). In the online appendix, we complement the empirical analysis with a three-sector behavioral New Keynesian DSGE model to illustrate the mechanisms underlying the food and energy price responses to weather shocks.

Our findings highlight several important points. First, distinguishing between hot and cold extremes is essential, as their effects on prices differ sharply. When seasonal effects are not accounted for, cold extremes raise food prices, while heat extremes lower them. For energy prices, cold spells have a modest upward impact, whereas hot extremes produce a more persistent decline that feeds through to headline inflation. Core inflation (excluding food and/or energy) shows little distinction between warm and cold shocks, underscoring that food and energy are the most temperature-sensitive components.

Seasonality further shapes these dynamics and provides a clearer picture. For food, winter and spring cold spells damage crops and raise prices, while warmer-than-usual conditions benefit production. In summer, heat extremes initially raise food prices, followed by a decline after several months—an S-shaped response consistent with demand effects found elsewhere in the literature. For energy, winter is the dominant season: unexpected cold winters increase prices, likely due to higher heating demand and reduced renewable generation, while warm winters have the opposite effect. Even after accounting for seasonal differences, energy prices remain the primary driver of headline inflation, given their economy-wide cost implications. While food prices have a smaller weight in Germany's CPI, we still find robust and significant responses across specifications. Robustness checks confirm that our results hold when using (renewable) energy output and consumption to disentangle supply and demand effects. Moreover, we find that the size of temperature shocks matters, revealing additional non-linearities in the price–temperature relationship.

In sum, our results suggest that central banks must take the inflationary implications of climate change seriously. Incorporating weather extremes into policy analysis is essential, as temperature fluctuations exert measurable and systematic effects on price dynamics.

The remainder of the paper is organized as follows. Section 2 reviews related literature. Section 3 describes the data and the identification of temperature shocks. Section 5 outlines the econometric framework, presents empirical results, and reports robustness exercises. Section 6 concludes.

2 Related literature

The empirical economic literature on the effects of climate change—through rising average temperatures and more frequent extreme weather events—on the economy and society has expanded substantially over the past 10–15 years. Much of this work focuses on traditional output measures such as GDP (see, e.g., Dell et al. 2012; Burke et al. 2015; Burke et al. 2018; Acevedo et al. 2020; Felbermayr and Gröschl 2014) and generally finds that extreme weather events or natural hazards reduce economic growth and harm production.[6] While early studies concentrated on warmer and poorer countries, more recent contributions increasingly document that advanced economies are also negatively affected by extreme weather. Within a panel local projection framework exploiting natural global temperature variability, Bilal and Känzig (2024) estimate global macroeconomic damages from climate change to be six times larger than previously thought. Berg et al. (2024) report negative GDP effects for a broad cross-section of countries, while Ciccarelli and Marotta (2024) find similar results for OECD economies. Kim et al. (2022) show that the U.S. economy experiences negative growth impacts from severe weather, accompanied by falling inflation.

Closely related to our focus on food prices, a large body of research establishes that rising temperatures reduce agricultural productivity and crop yields globally: Schlenker and Roberts (2009) for the United States, Schlenker and Lobell (2010) for Africa, Moore and Lobell (2015) for Europe, and Welch et al. (2010) for Asia. The impact of temperature on energy demand has also attracted growing attention (see Auffhammer and Mansur 2014), with evidence such as the U-shaped relationship documented by Deschênes and Greenstone

[6]For a comprehensive overview of this literature and its empirical approaches, see Dell et al. (2014).

(2011), whereby demand peaks on both very cold and very hot days, though the net effect varies across climate zones. For a broader review, including non-economic outcomes, see Carleton and Hsiang (2016).

By contrast, the literature on the effects of weather events and temperature extremes on price levels is relatively sparse. Regarding natural disasters, Parker (2018) find only limited price effects in advanced economies, while poorer countries experience substantial and persistent impacts, including rising food prices but declining inflation in other components. Evidence for temperature effects in developed countries is more mixed. Conceptually, our work is closest to Faccia et al. (2021), Ciccarelli et al. (2023), Kotz et al. (2024), and Lucidi et al. (2024). For a panel of 48 countries, Faccia et al. (2021) show that extreme warm temperatures, especially in summer, raise food prices in the short run, with prices falling in the medium term, and no significant effect on headline inflation. Using a panel of 121 countries, Kotz et al. (2024) confirm the strong food price response to positive temperature shocks and find spillovers to headline inflation, while other components remain largely unaffected. Lucidi et al. (2024) emphasize energy price responses in advanced economies, noting that higher temperatures reduce heating demand and energy prices, thereby lowering overall inflation, but that food prices tend to rise after hot spring or summer months. In a time-series framework for multiple European countries, Ciccarelli et al. (2023) find hot summers most strongly affect food prices in Southern Europe, while for Germany, effects are mostly insignificant or deflationary (e.g., for warm winters). All four studies highlight the importance of seasonal heterogeneity and non-linearities, and all measure temperature shocks as anomalies from historical averages.

We depart from this literature by adopting an alternative identification strategy inspired by Natoli (2023) to construct temperature shocks. While Natoli (2023) primarily examines macroeconomic impacts and finds an overall deflationary price response, we adapt and extend the approach to German data to provide new insights. This places our work within the

more technical literature on the identification and use of weather shocks. A related strand incorporates temperature levels or anomalies into structural VAR models, identifying shocks by ordering temperature first in a Cholesky decomposition, as in Donadelli et al. (2017).

3 Data and Construction of the Weather Shock

3.1 Climate data

For temperature data, we use the ERA5 reanalysis dataset (Hersbach et al. 2020), provided by the Climate Data Store (CDS) of Copernicus and the European Centre for Medium-Range Weather Forecasts (ECMWF). The dataset is available at an hourly frequency and offers a high spatial resolution of $0.1^\circ \times 0.1^\circ$ in both latitude and longitude. Coverage begins in 1950 for most countries worldwide and extends to the present day. The processing and aggregation steps are described in detail in the following sections. The major advantage of this type of reanalysis dataset is that it integrates climate model simulations with observed meteorological data into a single, consistent framework. Climate models are used to interpolate between weather stations, thereby improving the precision and reliability of the granular data. An alternative would be so-called gridded datasets, which primarily rely on statistical methods for interpolation between ground stations.[7] We rely on ERA5 because it is widely used in recent econometric applications and offers high geographical resolution, enabling us to identify our shock measure at the most regional level possible. For robustness exercises, we also include aggregated sunshine duration and precipitation for the whole of Germany, obtained from the Deutscher Wetterdienst (DWD).

3.2 Macroeconomic and regional data

The main source for our macroeconomic (price) data is Eurostat, for two reasons. First, from 1996 onward, it provides continuous monthly data on prices in the form of the Harmonised Index of Consumer Prices (HICP) for Germany and other European Union countries. This

[7] Auffhammer et al. (2013) shows a high correlation between reanalysis and gridded data for temperatures.

index is a standardized measure, which makes it easy to compare price developments both across and within countries. Hence, the analysis can easily be applied to other countries as well. Second, by design, the HICP consists of five main components (and many more sub-components): unprocessed food, processed food, energy, non-energy industrial goods, and services. According to the European Central Bank, this breakdown is based on the idea that each component tends to comprise items related either to their use or their production, and thus to the factors affecting their developments. For example, energy and unprocessed food are mainly influenced in the short term by exogenous factors (such as weather), whereas the other components are less volatile and are more affected by domestic economic factors (e.g., wages or margins). Examining these components separately allows us to better understand the mechanisms underlying price changes. We use data for the five components and the overall HICP for Germany, starting in January 1996. The sample ends in December 2021, excluding 2022 and 2023 due to the prevailing energy crisis in Europe. Thus, we analyze the effect of temperatures on inflation for a period of relatively stable price levels.[8] We apply a seasonal adjustment procedure (X-13ARIMA-SEATS Seasonal Adjustment Program) to all price indices, which are otherwise unadjusted. This is an additional step to account for seasonal patterns unrelated to weather extremes. In addition, we use the industrial production index as a control variable, with monthly data from Eurostat. Monetary policy rates are obtained from the FRED database, also at a monthly frequency. For periods when the policy rate reached the zero lower bound, we use the shadow rate from Wu and Xia (2017) and Wu and Xia (2020). Thus, the monetary policy rate in our econometric model combines the standard rate and the shadow rate. Regional (county-level) data used for aggregating our weather shocks come from the INKAR database. For robustness checks, additional specifications include data on renewable energy production and consumption from the Agorameter database, as well as information on Germany's growing season from the

[8]Excluding the years 2020 and 2021 because of Covid does not materially change the results.

World Bank. An overview of all variables and data sources is provided in Table 9 in the appendix 7.13.

3.3 The construction of the weather shock

3.3.1 The Problem with Temperature Shocks

Before turning to our shock design, it is important to explain why temperature is preferred over other weather indicators when quantifying the economic impact of weather and global warming. One primary reason is that temperature data are systematically recorded at a continuous and high-frequency basis. The availability of such granular data enables straightforward computation of temperature statistics with a high degree of geographical precision. These properties make temperature a more suitable choice than other extreme weather events, such as hurricanes, floods, or earthquakes. The importance of identifying a well-designed temperature shock arises from the fact that both the annual German average temperature and the price index have trended upward over our sample period. This complicates the identification of the true causal effect of weather on the price level. A simple regression of prices on temperature levels would reveal a spuriously positive association, as argued by Bilal and Känzig (2024). This makes shock construction a central element of our paper. As noted in Section 2, many studies identify temperature shocks using temperature anomalies—deviations from long-term averages—and then estimate their effects on other variables. This approach helps isolate departures from typical conditions, making unusual patterns or extremes easier to detect. However, as Natoli (2023) point out, relying on anomalies defined relative to pre-sample means has several limitations. First, the use of (monthly, quarterly, or yearly) temperature averages risks smoothing out extremes. For instance, if a month begins with several hot days and ends with several cold days, the monthly average temperature may appear normal, even though the period experienced two opposite extremes. Second, a related problem arises in spatial aggregation: because temperature can vary substantially over short distances, averaging across regions risks obscuring

local extremes. Third, agents may be aware that the temperature distribution is shifting over time. As a result, deviations from long-past historical means may not be perceived as unusual and would therefore fail to qualify as true shocks. Another approach in the literature[9] is to count the number of days within a given period (month, quarter, or year) when the average daily temperature exceeds (or falls below) a predefined threshold, such as 30 °C. This allows short-lived extremes to be captured—events that would be averaged away under the anomaly method. This idea forms the basis of our own shock construction. However, this approach also has limitations. Defining an appropriate threshold is more complex than it appears. In Germany, for example, a threshold of 30 °C may be sensible for summer, when such temperatures are possible and considered unusually hot. But in autumn, winter, or spring, daily temperatures rarely, if ever, exceed that threshold. Different thresholds would therefore be needed for each season, which are difficult to determine ex ante—especially for transitional seasons such as spring and autumn.

Since our analysis works at the monthly frequency, distinguishing between seasons and capturing their nonlinear effects is a key part of our design. Consequently, we apply season-specific thresholds, which is particularly important in the context of a changing climate.

3.3.2 Our approach

Our approach builds on the work of Natoli (2023), who constructed his shock measure for the U.S., and adapts it for Germany as explained below. Specifically, we let the data speak for itself by determining thresholds based on the distribution of temperatures over time. We begin with hourly data and aggregate it to the daily level, working at the most granular regional level possible—German Landkreise (counties). In this way, we account for regional weather phenomena in our shock measure before aggregating it to the macro level (weighted average). Fortunately, the ERA5 dataset (Hersbach et al. 2020) has a horizontal resolution of

[9]See, for example, Dell et al. (2014).

$0.1^\circ \times 0.1^\circ$.[10] We assign each coordinate point to its respective Landkreis using geographical data from the GADM database. For each Landkreis, we then create a daily time series by averaging all observations corresponding to that region for each day. Next, we count the number of days within each month, for each region, on which the average daily temperature exceeds or falls below a specific dynamic threshold. The novelty of this approach lies in the way these thresholds are determined. To classify a day as an extreme (hot or cold), we use temperature values from the same month over the previous five years as a reference. A day is defined as extreme if its temperature lies above the 90th percentile or below the 10th percentile of the reference distribution.[11] This ensures season-specific thresholds throughout the year. The rationale for using a rolling reference window is as follows: most people are aware that temperatures are rising and that extreme weather events are becoming more frequent. For example, the average summer between 2016–2020 is warmer than between 1976–1980, and most agents know this, adjusting their expectations accordingly. Using a reference period far in the past would therefore misrepresent agents' beliefs and overestimate the incidence and size of shocks, which in reality may not be surprising to them at all. Our rolling window approach avoids these problems and models agents' expectations at the same time. A five-year window[12] seems appropriate, as the literature suggests it takes multiple years for beliefs about global warming to update (Deryugina 2013; Choi et al. 2020). At the same time, the window is short enough to avoid the distortions just discussed. By incorporating this Bayesian learning mechanism into our shock construction, we ensure the shocks represent genuinely unexpected—and therefore exogenous—temperature variations. While we largely follow Natoli (2023), we have made several adjustments for the German context. Most notably, we work with monthly rather than quarterly data. One argument for

[10] We take the westernmost to the easternmost points of Germany, and similarly the northernmost to the southernmost, to cover the full territory. All coordinate points outside Germany are excluded.

[11] For example, the complete reference distribution for January consists of $5 \times 31 = 155$ January days from the past five years.

[12] We conducted robustness checks with different window lengths; results remained unchanged.

quarterly data is that, within a quarter, firms may adapt and reschedule activities to mitigate the impact of extreme events. Moreover, macroeconomic aggregates like GDP are reported quarterly and roughly align with calendar seasons. However, for our purposes, a monthly series has a clear advantage: when constructing quarterly shocks—defined as the number of days in a quarter that are unusually hot or cold—one must compare temperature values from different months or even different seasons. Take winter as an example: January, February, and March. From a meteorological perspective, March is already spring, and its average temperature is higher than January's. Relatively warm days in January might therefore be classified as average when compared with March, and would not be counted as shocks. As a result, their effects on economic variables could be missed entirely. We observe this issue clearly in the data: at the regional level, nearly 70% of warm days in first-quarter (winter) shocks occur in March, while only 13% occur in January and 19% in February. Similar patterns hold across other seasons. This supports the argument that quarterly shocks fail to capture month-specific extremes, producing a series that does not fully represent the underlying dynamics. Furthermore, because our study focuses on price developments—and the consumer price index is reported monthly—the rationale for quarterly data does not apply. Using monthly shocks ensures greater precision and alignment between the weather shock measure and the price data.

What remains is to translate the preceding ideas into a formal framework that explicitly incorporates expectations. Expectations are crucial because, in a general setting, a shock—here defined at the regional level—can be represented as the deviation of the actual observed temperature statistic from its expected value; in other words, the shock corresponds to the temperature expectation error:

$$f(T_t^i) - E_{t-1} f(T_t^i) \tag{1}$$

In equation (1), $f(T_t^i)$ is the observed temperature metric for "Landkreis" $i = 1, ..., k$ in

month t, in our case the number of days, which are categorized as hot or cold, while the second term is the previous formed expectation for that value. Using the reference distribution, the monthly upper (ut) and lower (lt) thresholds when forming expectations are determined as follows.

$$ut(m)_y^i = F_{m,y}^{-1}(0.9) \qquad \forall \qquad m = \{01, 02, ..., 12\} \tag{2}$$

$$lt(m)_y^i = F_{m,y}^{-1}(0.1) \qquad \forall \qquad m = \{01, 02, ..., 12\} \tag{3}$$

$F_{m,y} = \{T_{d,m,y-j}^i, j = 1, ..., 5\}$ is the empirical cumulative distribution function of the reference temperature distribution for month m and year y, where $T_{d,m,y-j}^i$ is the average daily temperature on day d, in month m and year y for "Landkreis" i. Its inverse $F_{m,y}^{-1}(x)$ provides the respective percentiles. One can easily combine these thresholds by month to get a monthly series for each "Landkreis" i, where t now indicates monthly frequency.

$$ut_t^i = \{ut(m)_y^i, m = 01, 02, ..., 12\}$$

$$lt_t^i = \{lt(m)_y^i, m = 01, 02, ..., 12\}$$

With these thresholds at hand, it becomes straightforward to determine the respective number of extreme days. However, there is another important point to have in mind. By design, agents classify 20% of each month to be extreme (10% extreme hot and 10% extreme cold), which we have to take into account when calculating the shock value by subtracting them. In addition, the reference distribution includes roughly 150 days, which need to be rescaled to a single month. Equations (4) and (5) formalize the described procedure to determine the shocks at the county level. Note that n_t is the number of days of the month for which the shock is calculated, while N_t displays the number of days of the whole reference window.

$$heat\_shock\_county_t^i = \sum_{d=1}^{n_t} I(T_{d,t}^i > ut_t^i) - \underbrace{N_t \times 0.1 \times 0.2}_{\text{Expectations}} \tag{4}$$

$$cold\_shock\_county_t^i = \sum_{d=1}^{n_t} I(T_{d,t}^i < lt_t^i) - \underbrace{N_t \times 0.1 \times 0.2}_{\text{Expectations}} \tag{5}$$

Here, $I(x)$ is an indicator function stating whether statement x is true or not, taking the values one and zero. $\sum_{d=1}^{n_t} I(T_{d,t}^i > ut_t^i)$ stands exemplary for $f(T_t^i)$ from equation (1), while $N_t \times 0.1 \times 0.2$ represents expectations. Thus, equations (4) and (5) can be seen as the empirical counterparts of the temperature expectation error from equation (1).

While regional climate variation could, in principle, be informative, systematic and comparable regional (food and energy) granular price data for Germany are not available. Moreover, food and energy markets are highly integrated, so regional shocks quickly pass through to national prices, which are the policy-relevant measure for the design of monetary policy. Regional heterogeneity would therefore add noise and confounding factors rather than sharpen identification. We therefore aggregate these local shocks to the macro level.

To achieve this, we collect population data at the "Landkreis" level to construct weights for each region. For aggregation, we calculate the weighted average of our local shocks and use it as the macro weather shock for Germany. The reason why population values are used as a weighting is the common assumption that the more people live in a region, the more people are exposed to these temperatures, and the stronger the effect on the economy. Alternatively, we construct weights based on agricultural variables. Neither the shock series itself nor the impulse responses estimated below change much qualitatively.

$$DEU\_heat\_shock_t = \sum_{i=1}^{L} (heat\_shock\_county_t^i \times w_t^i) \tag{6}$$

$$DEU\_cold\_shock_t = \sum_{i=1}^{L} (cold\_shock\_county_t^i \times w_t^i) \tag{7}$$

Theoretically, and as suggested by Natoli (2023), the combined general temperature shock at the macro level is then simply the sum of $DEU_heat_shock_t$ and $DEU_cold_shock_t$, assuming

Figure 2: Nationwide temperature shock for Germany.

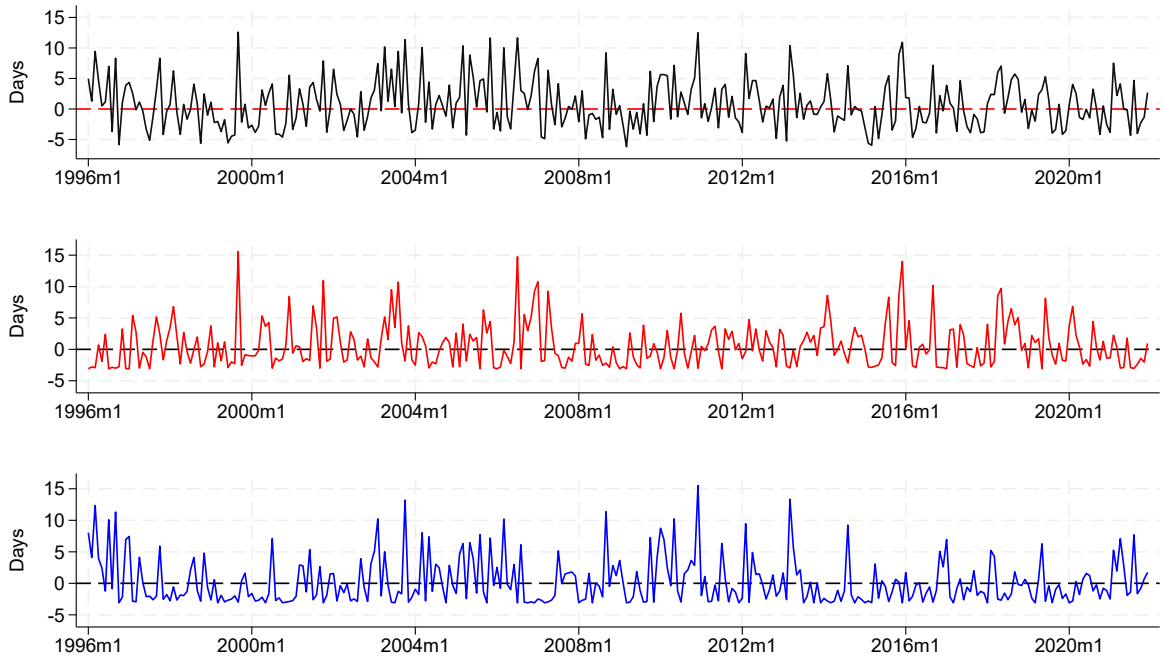

that hot and cold temperatures are undesirable to the same extent:

$$DEU_shock_t = DEU_heat_shock_t + DEU_cold_shock_t \tag{8}$$

However, simply summing the hot and cold shocks leads to a biased representation of the underlying weather situation as argued below.

3.4 The weather shock: Challenges and insights

Figure 2 shows the aggregated shock series for Germany for all three types: the combined shock, as well as hot and cold days separately. The combined shock has a minimum of −6.1959, and its maximum is 12.6129. The mean is positive with 0.79 and significantly different from zero[13]. At this point, it is useful to discuss the general interpretation of the shock, bearing in mind potential weaknesses. Most importantly, a positive value does

[13]Confidence level of 99%.

Figure 3: Composition of the combined shock for different sample months.

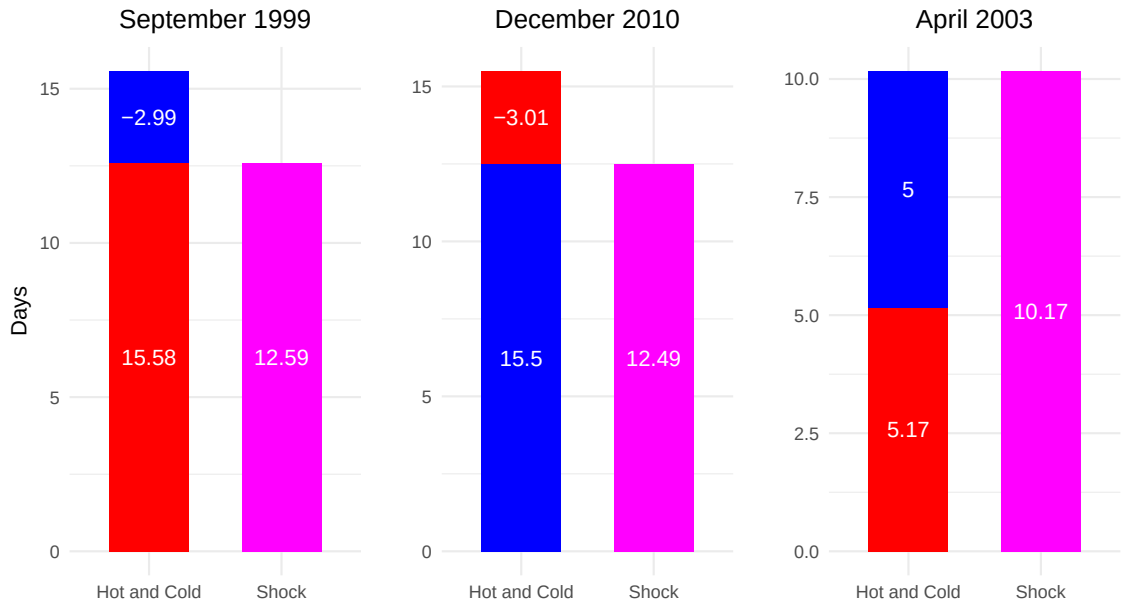

not necessarily mean a warm temperature shock. It just states that temperatures in a particular month were surprising for the agents, which can be particularly hot, but also particularly cold (or both). This is due to the fact that hot and cold days are simply added up. In general, a negative value can be interpreted as "milder" temperatures than expected, which might be favorable for agents and the economy, while a positive value is undesirable. However, particularly in months where the shock value for one of the extremes becomes negative (which is possible due to expectations), there is a considerable risk that the two extremes offset each other, distorting the overall shock value. To get a better idea, let us take a look at figure 3, where the different numbers for each shock type are plotted for three chosen months. Looking at September 1999 (left plot), one can observe a large shock value for hot days (15.58). In the same month, the value for cold days is negative (-2.99). Consequently, the combined shock amounts to 12.59. This indicates that the big shock value is driven solely by the unusually warm month, while the inclusion of the cold day component actually reduces the overall value. So the question arises as to whether the combined shock

represents how things looked in terms of temperature this month. In December 2010, one can observe the opposite. We have a larger number of cold days $(15, 50)$, while for warm days, the sign is negative (-3.01). Hence, the combined shock is $12, 49$. A similar value as in the example before, but the observed temperature phenomena is the complete opposite. Thus, the composition of the combined temperature shock (sum of hot and cold days) does change during the sample. Sometimes, hot spells dominate, while other times, cold spells take precedence, meaning the same observation value can represent two entirely different phenomena, which this type of shock cannot adequately distinguish. The right plot of figure 3 shows a third example, where heat and cold extremes are even. Hence, another possible shock composition. On top of this, the values might cancel each other out, as argued above. In fact, the problem of different signs is omnipresent for our sample, as the sign of heat and cold shocks is different 62.18 percent of the time. This complicates the task of tracking the true effect of weather events on the economy. Is the response of a variable because of a hot or cold extreme? Those and other questions can only be answered if we distinguish between warm and cold temperature extremes. All this even becomes more problematic over time due to climate change, where extreme periods happen more often while at the same time, temperature fluctuations increase. Thus, from now on, we will focus on hot and cold days separately and include them both in our local projection analysis. As presented in table 1

Table 1: Summary Statistics for Temperature Shocks

						Ljung-Box test	
	T	Mean	SD	Min	Max	Q-stat	p-value
Combined Shock	312	0.78	4.02	−6.17	12.59	16.43	0.87
Hot Days	312	0.58	3.50	−3.09	15.58	28.43	0.24
Cold Days	312	0.20	3.69	−3.09	15.50	30.73	0.16

for hot days, the mean is 0.58 and significantly different from zero. For cold days, this is not the case with a mean of 0.21. Hence, both means are smaller than for the combined shock.

Regarding the standard deviation, it is smaller as well, while it is still comparable for all three shocks. The maxima are larger for the individual shock types, which does not come as a surprise since there is no risk of hot and cold canceling each other out. The minimum is the same for both, which is given by construction.[14] This is why it is the same for both and occurring multiple times during our sample. The last two columns of table 1 present the results of a Ljung-Box test for serial correlation. All three types of shock do not show a pattern of autocorrelation, as the null hypotheses of zero autocorrelation cannot be rejected at the five percent level.

Further, the distinction by season is essential. The assumption of hot and cold temperatures being equally bad for humans and the economy might be not as justified as thought, as we argue it strongly depends on the season what temperatures or what kind of shocks might be desirable.[15] For example, a rather cold summer might be quite decent for humans, especially in times of rising global temperatures. In the same manner, a warm winter might be favorable in terms of heating and energy costs. This is why in the local projection framework below, we include season dummies and their interactions with temperatures in the model. Table 2 shows additional descriptive statistics by season. For that, we take only months into account for which the number of extremely hot or cold days is positive and classify them by calendar seasons. Overall, we find 146 months during our sample where the number of hot days is positive. The distribution between the seasons is relatively even, with each season accounting for around a quarter of the extreme months. Interestingly, for winter and summer averages are the largest, with 3.90 days per month in winter and 3.97 for summer. Highlighting that for these seasons where the temperatures are most extreme in levels, the hot surprises are most prominent. At the same time, we count 114 months where

[14] If one has zero extreme days for one month, one simply subtracts $155 \times 0.2 \times 0.1 = 3.1$. It is the number of expected extreme days (hot or cold) per month for months with 31 days.

[15] The fact that the calendar season has implications for the effect on the economy is also found in Kotz et al. (2024) or Faccia et al. (2021).

the number of cold days is positive. Consequently, months with warm extremes are more frequent than months having cold extremes. As before, the distribution between seasons is relatively even. The average values are highest for spring and winter.

Table 2: Temperature Shock and Seasons

Positive number of hot days								
Total	Fall		Winter		Spring		Summer	
	%	Days	%	Days	%	Days	%	Days
146	26.7	3.26	24.7	3.90	26	2.92	22.6	3.97
Positive number of cold days								
Total	Fall		Winter		Spring		Summer	
	%	Days	%	Days	%	Days	%	Days
114	24.6	3.60	26.3	4.45	28.1	4.40	21.1	3.94

As a last step, we compare our shock to the most used measure in the literature, namely temperature anomalies.[16] To make it comparable to our shock, we use the most recent five years as the reference period, instead of a pre-sample period. Hence, we have a similar type of learning behavior included as before. We use our dataset to compute these temperature anomalies on the regional level and then aggregate them in the same way as we aggregated our shocks above. The correlation between anomalies and our shocks is strong and significant for both types (0.76 for hot and -0.78 for cold days). The strong correlation with this type of shock supports the usage of our counting method and differentiates between hot and cold extremes. At the same time, our method provides the added benefit of preserving the impact of opposite extremes within a month rather than canceling them out. To conclude, by looking at the characteristics of the shock and comparing it to alternatives from the literature, it seems important for us to discriminate between hot and cold shocks, especially when taking into account the problem of negative values when taking the sum. At the same time, we have

[16] See references from section 2.

to account for the different consequences of temperature extremes during different seasons over the year. Therefore, in section 5, we proceed by using both shocks (hot and cold extremes) separately in our analysis and let them interact with season variables.

4 Identifying assumption

To support the claim that the estimated responses to our shocks genuinely reflect the causal effect of temperature on prices, we aim to demonstrate that these shocks are exogenous with respect to the dependent variable. To do this, we break down the underlying empirical problem, following the approaches of Hsiang (2016) and Hsiang et al. (2013).

Researchers need to distinguish between two hypotheses: the null hypothesis, that climate has no impact on prices, and the alternative, that climate has a significant impact. This distinction is complicated by the high dimensionality of both climate and economic processes, which introduces many potential confounding factors. In an ideal experimental setup, we would observe two identical countries, apply the treatment (extreme temperature) to one, and use the other as a control. Since such an experiment is not feasible, we instead rely on natural variation in climate-specifically, variation that is independent of other factors influencing prices.

As already noted, we deliberately avoid a cross-sectional approach. Methodologically, we reconstruct the historical physical exposure of each population to climate conditions and estimate the effect of temporal variation using standard econometric techniques. Our identification strategy relies on the assumption that each population is comparable to itself over time, effectively allowing each unit to serve as both treatment and control. By avoiding cross-sectional comparisons, we further reduce the risk of omitted variable bias. Countries differ in many respects, including supply chains, agricultural structures, institutional settings, and—most importantly—climatic zones, many of which are unobservable. These omitted factors could easily confound a cross-country analysis, making treatment and control groups incomparable and thereby undermining causal inference.

Additional sources of omitted variable bias-such as domestic policy responses, behavioral changes, or structural economic adjustments-tend to evolve over longer time horizons. As our data are at monthly frequency, these slower-moving factors are unlikely to bias our contemporaneous estimates. The high temporal resolution of our analysis plays a key role in limiting the potential for short-term confounding. For the same reason, we avoid including an excessive number of control variables in our model. Including controls that are themselves influenced by climate can introduce problems known as "bad control" (Angrist and Pischke 2009) or "overcontrolling" (Dell et al. 2014). This occurs when the control variable absorbs part of the true climate effect or introduces spurious bias by correlating with unobserved population differences that are, in turn, linked to climate variation.

A second classical source of endogeneity is reverse causality. In our case, this concern is mitigated by using pre-constructed weather shocks. These rely on the standard identification assumption that weather patterns, being governed by geophysical processes, are exogenous to economic activity, and therefore unaffected by price dynamics. As with other weather-related phenomena, temperature fluctuations occur randomly over time and can thus be regarded as exogenous to both current and prior economic outcomes, at least in the short term. This helps preserve the validity of our identification strategy.

To support this claim, we test whether our shock measures can be predicted based on past price information, as Bilal and Känzig (2024) do for their shock design. Specifically, we estimate bivariate vector autoregressions (including up to six lags of each temperature shock and inflation rates for various price categories) and conduct Granger causality tests. The results, shown in Table 3, indicate that the null hypothesis of no Granger causality is generally not rejected. This suggests that the temperature shocks are not predictable from the included price variables. In the case of energy inflation, where the p-value approaches the 10% threshold of statistical significance, the economic importance appears limited. The effect is not stable across lag specifications, and there is no clear causal mechanism by which energy

prices should predict weather extremes, particularly since our shock construction removes seasonal variation by design.

Given these considerations, we argue that our empirical estimates can be interpreted as

Table 3: Predictability of the shock series – Granger causality tests

		Inflation	Food Inflation	Energy Inflation
Combined Shock	χ^2	4.04	5.88	10.38
	$p(\chi^2)$	0.671	0.44	0.11
Hot Days	χ^2	9.17	4.60	10.19
	$p(\chi^2)$	0.16	0.60	0.12
Cold Days	χ^2	7.85	4.16	10.72
	$p(\chi^2)$	0.25	0.66	0.10

identifying the short-run causal impact of unanticipated weather shocks on aggregate price levels. The aggregation over time and across sectors, which is inherent in monthly data, combined with the natural inertia of most economic adjustment processes, strengthens the validity of the exogeneity assumption at this temporal resolution. The design of our shock variable is therefore robust for estimating the causal effects of weather variability on prices. In summary, all of our shock types satisfy the three key criteria for identifying shocks in macroeconometric analyses, as outlined by Ramey (2016): (i), they are exogenous with respect to current and lagged endogenous variables; (ii) they are uncorrelated with other exogenous shocks; and (iii) they represent unanticipated changes in an exogenous variable.

5 Econometric Framework and Empirical Evidence

5.1 Hot versus cold weather periods

We estimate the impulse response functions (IRF) of multiple economic variables to our constructed shock measures using the local projection framework of Jordà (2005). Since we have already identified an exogenous shock and aim to track its dynamic effects on our endogenous variables, this method proves highly suitable for the analysis. Its great flexibility allows us to easily incorporate non-linearities. Furthermore, according to Ramey (2016) this

estimation method is more robust to miss specifications of the model compared to other standard approaches such as VAR models. To obtain typical IRFs, we conduct a series of separate time series regressions for multiple horizons $h = 0, ..., H$. This approach estimates the effect on the endogenous variable at various points in time following the shock, with the respective coefficients at each horizon forming the IRF. Equation 9 shows our baseline model.

$$ln(y_{t+h}) - ln(y_{t-1}) = \alpha_h + \beta_h \text{hot\_shock}_t + \gamma_h \text{cold\_shock}_t + \sum_{l=1}^{12} \delta_{h,l} \mathbf{X_{t-1}} + \phi_h t + \psi_h t^2 + \epsilon_{t+h} \quad (9)$$

We apply this model to multiple components of the HICP, while the dependent variable is the cumulative growth of the respective component.[17] By that we ensure estimating a possibly persistent level effect. We include both of our identified shocks separately in our regression. Then the main coefficients of interest are the β_hs and γ_hs forming the IRFs. We further include a small set of control variables (respectively, their lags) in the vector $\mathbf{X_t}$. Those are the year on year growth rate of industrial production in Germany, the monetary policy rate, and lags of the growth rate (inflation rate) of the dependent variable. We include lags up to one year. In addition, we use time and quadratic time trends. For all estimations, we use New-West standard errors, since in such a time series framework the error terms ϵ_{t+h} are always serially correlated, except for horizon $h = 0$.[18]

Figure 4 displays the impulse response functions to a one–standard-deviation shock for various components of the HICP, including the overall index (all items), non-processed food, energy, and the core index, which excludes both food and energy. The focus on these four indices stems from the literature, which suggests that food and energy items are particularly

[17] Before performing the empirical analysis, we seasonally adjust the CPI data using standard methods. However, to ensure that this procedure is not driving our results, we perform the same empirical analysis using year-on-year inflation rates, another possibility to exclude seasonal effects. The results remain robust and are reported in the online appendix.

[18] For details see Ramey (2016).

Figure 4: Impulse response functions for different components of the harmonised index of consumer prices, separately for hot temperature shocks (red) and cold temperature shocks (blue). The respective shaded areas represent 68% confidence intervals computed using Newey–West standard errors.

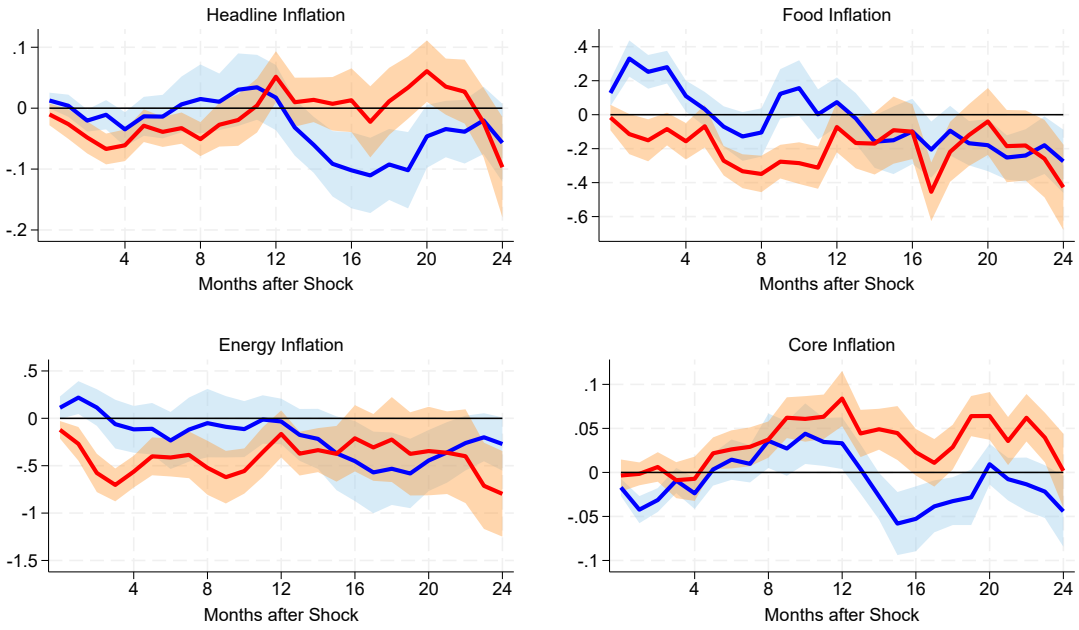

sensitive to climatic conditions and generally exhibit the highest volatility. In particular, non-processed food (wheat, fruits, vegetables, etc.) is likely to be strongly affected by weather events. To assess their impact on the overall price level and observe the reaction without them, we also examine the other two components (headline and core inflation). Starting with headline inflation in figure 4, the response for the warm shock type is rather deflationary, while there is almost no response for cold extremes. The decrease in the overall price level is significant and persists for roughly a year after the shock. To get a fist clue of what is driving this result, we have to look at energy and food prices (first row, second column and second row, first column in figure 4). For hot extremes, the response of energy is significantly negative throughout the whole horizon and of large magnitude (almost 1 percent), while for cold ones, there is no reaction at all. It seems to be similar to food prices, except that cold periods lead to short-term price increases. At first, this result comes as a bit of a surprise,

as the literature states that hot summers cause damage in agriculture, leading to increased food prices. However, the picture becomes clearer when focusing on the different seasons below. For core inflation, we do not see any significant differences nor responses for both the hot and cold shocks, confirming that food and energy are probably the most affected sectors, which drive the response of overall inflation. It is important to note that the reactions to hot and cold extremes tend to be opposite (at least on impact and following months), except for core inflation. This further reinforces our earlier argument that distinguishing between the two types of shocks is crucial, as simply aggregating them distorts the results. Nevertheless, to understand why warm spells lead to a decrease in energy prices and cold extremes drive an increase in food prices, it is essential to differentiate between the four seasons of the year in order to uncover the causal mechanisms behind these effects.

5.2 Do seasons matter?

As argued above, it seems likely that an exceptionally hot month in summer has a different effect than exceptionally warm months in winter. This is why we decided on another model specification, accounting for different seasons in equation 10.

$$ln(y_{t+h}) - ln(y_{t-1}) = \alpha_h + \sum_{j=1}^{4} (\beta_h^j \text{hot\_shock}_t \times D_t^j + \gamma_h^j \text{cold\_shock}_t \times D_t^j) + \sum_{l=1}^{12} \delta_{h,l} \mathbf{X_{t-1}} + \phi_h t + \psi_h t^2 + \epsilon_{t+h} \tag{10}$$

We include each season in the regression by interacting it with our two temperature shocks. To translate this formally into our empirical model, we add the dummy variables D_t^j, with $j \in 1, 2, 3, 4$, which take the value one if the current month is in season j of the year and zero otherwise. The respective IRFs then consist of the coefficients β_h^j and γ_h^j. Building on our econometric framework, we compute impulse responses once more, distinguishing between hot (red line) and cold (blue line) temperature extremes. The following subsections offer a detailed analysis of the impulse responses for non-processed food, energy, headline, service, and core inflation, broken down by different seasons.

5.2.1 Food prices

We start our analysis by looking at impact effects (and the subsequent quarter) of our shocks on food prices in table 4. Afterwards, we also further check the persistence of those effects by focusing on the medium-term responses of the dependent variable. On impact, we see various significant effects of our temperature shocks on food inflation, with clear seasonal heterogeneity. Most notably, hot summers lead to significant increases in food inflation in the months following the shock, with the strongest and most significant effects observed one and two months after the initial shock (0.30 and 0.39 percentage points, respectively). This is in line with the previously presumed negative impact of heat on food production, especially during summer, which likely translates into rising prices through supply-side constraints. By contrast, hot winters have the opposite effect, leading to a delayed but significant decline in food inflation from month one onward, reaching -0.51 percentage points at horizon 2. This pattern suggests that warmer winter temperatures may ease agricultural production conditions or might reduce storage and transport costs, ultimately lowering food prices. Similar, though slightly less robust, downward effects are visible following hot spring and hot fall shocks. Turning to cold shocks, the most pronounced effect appears for cold springs, which are associated with a significant increase in food inflation—up to 0.68 percentage points by month 3. This likely reflects frost-related damages or delayed growing conditions affecting supply, a result often found in the literature.[19] Cold shocks in other seasons, however, produce less consistent and mostly insignificant effects. Taken together, these results indicate that temperature extremes, particularly heat in summer and cold in spring, have non-trivial and directionally consistent effects on food prices in the short term.

To assess whether these effects are merely short-lived or exhibit greater persistence, we next turn to the impulse response functions shown in figure 5. These plots extend the

[19] Hatfield and Prueger (2015) and Auffhammer and Schlenker (2014) and the references therein document that cold periods could lead to a reduction of crop yields.

Table 4: Effects on Impact for Food Prices

	Food Inflation			
	Horizon 0	Horizon 1	Horizon 2	Horizon 3
Hot Winter	-0.11	-0.40*	-0.51***	-0.36**
	(0.13)	(0.22)	(0.18)	(0.18)
Hot Spring	-0.03	-0.16	-0.32*	-0.30
	(0.13)	(0.21)	(0.19)	(0.21)
Hot Summer	0.07	0.30***	0.39***	0.29*
	(0.07)	(0.11)	(0.12)	(0.15)
Hot Fall	-0.04	-0.33	-0.40*	-0.20
	(0.14)	(0.21)	(0.22)	(0.21)
Cold Winter	0.07	0.28	0.29	0.10
	(0.16)	(0.21)	(0.20)	(0.22)
Cold Spring	0.24	0.50**	0.58**	0.68**
	(0.15)	(0.20)	(0.24)	(0.27)
Cold Summer	0.08	0.24	-0.04	0.08
	(0.13)	0.17)	(0.20)	(0.22)
Cold Fall	0.04	0.16	-0.17	-0.02
	(0.15)	(0.19)	(0.18)	(0.21)
Time Trends	Yes	Yes	Yes	Yes
Observations	288	287	286	285
R^2	0.26	0.36	0.38	0.38

Newey-West standard errors in parentheses

* $p < 0.10$, ** $p < 0.05$, *** $p < 0.01$

analysis to a 24-month horizon, allowing us to trace the medium-term dynamics of food price responses to seasonal temperature shocks. Also in the medium-term several clear patterns emerge, highlighting notable asymmetries in both magnitude and persistence across seasons and shock types. Starting with fall shocks (top left panel), we observe that hot fall periods lead to persistent deflationary pressure on food prices, reaching a trough of roughly -0.5 percentage points around month seven. This suggests that mild fall conditions, possibly associated with extended harvesting periods or improved storage conditions, may ease supply constraints. The deflationary impact is somewhat mirrored by cold fall shocks, which also lead to falling prices, though with greater persistence and slightly larger effects beyond month 12. These results may reflect the transitional character of fall, where both hot and cold deviations can affect harvest timing and labor productivity in different ways. For winter shocks (top right panel), we obviously still see that warm winters result in a short-term decrease in food prices. However, cold winters produce a rather short-lived and

modest inflationary impulse, peaking around month 2 and then quickly fading—suggesting that such a shock causes no persistent response, as the effects for both types of shocks are not different from zero in the periods afterwards. Taken together, these findings are in contrast to Ciccarelli et al. (2023), that do not find any significant impact of weather shocks on unprocessed food data for the fall and winter periods in Germany. At the same time, the authors report similar effects for other European countries, such as France and Italy, lending further support to the mechanisms discussed above.

Figure 5: Impulse response functions for the unprocessed food component of the harmonized index of consumer prices, shown separately for hot temperature shocks (red) and cold temperature shocks (blue), presented for each calendar season. The respective shaded areas represent 68% confidence intervals computed using Newey–West standard errors.

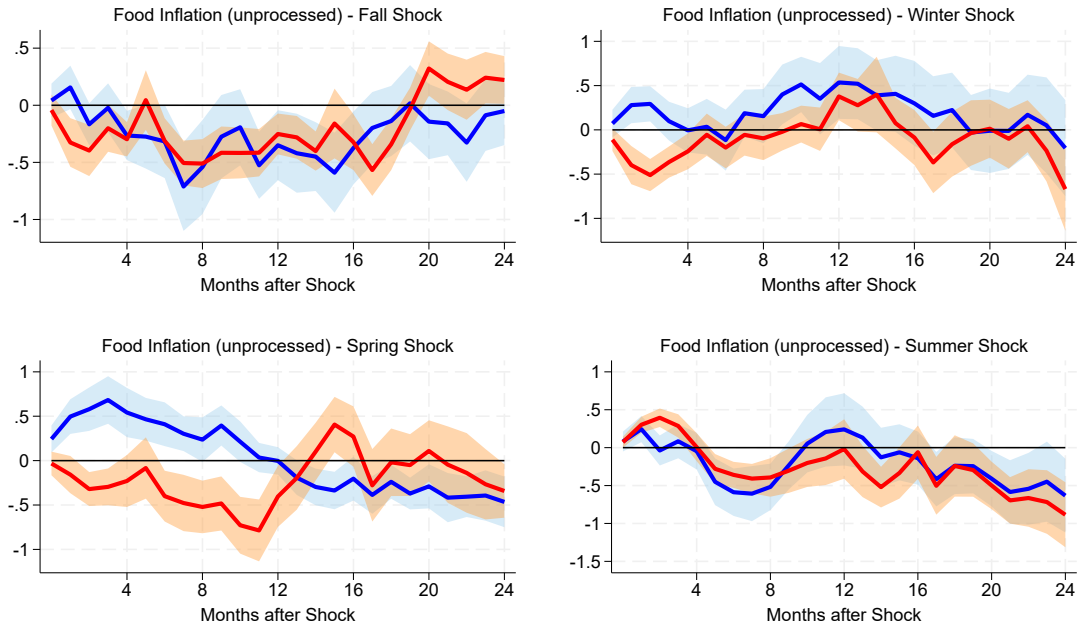

Turning to the spring period (bottom left), we find clear evidence of asymmetric effects. Hot spring periods result in a sustained decline in food inflation, lasting up to 13 months. This is consistent with improved growing conditions due to warm temperatures. Such warm spring periods are favorable for the growth process of many fruits and vegetables that yield to higher agricultural output and lead to a consumer price reduction. In contrast, cold

spring shocks cause a prolonged and significant increase in food prices, reaching up to 0.5 percentage points and persisting beyond one year. These findings for the medium-run confirm that cold springs hinder early growth phases of crops and reduce yields, as already discussed above. In cold and presumably wet seasons during spring, the growth process of plants is affected by bacterial diseases and fungal infections, leading to crop failures throughout the year. This also holds true for the wet or cold summer seasons (bottom right), where harvesting periods are negatively affected by rainy and cold weather conditions. However, the effect is smaller and less persistent than for the spring periods. This observation is in line with the finding of Crofils et al. (2025) arguing that the distinction between growing and harvesting seasons plays an important role in production in the agricultural sector. For Peruvian data, the authors show that there is a stronger reduction in agricultural production when a shock occurs during the growing season. Finally, the hot summer shock (also bottom right) shows a short-lived but sharp increase in food inflation, peaking at 0.5 percentage points two months after the shock (as shown in table 4), before returning to baseline levels around month five. This humped-shaped pattern reflects harvest-related vulnerabilities. It is well-documented that there is a negative correlation between warmer temperatures and outdoor labor productivity (Dasgupta et al. (2021)) that, for a given growth process, further reduces agricultural production. This humped-shaped behavior is similar to the findings by Faccia et al. (2021), Lucidi et al. (2024) or partly Kotz et al. (2024) and can also probably be explained by demand effects, which come into play after the price increase, causing the following decrease. Hence, the observed increase is only temporary and not persistent over the medium-run.

5.2.2 Energy prices

Figure 6 and table 5 present the estimated effects of seasonal temperature shocks on energy inflation in the short- and medium-term.

As with food prices, we observe significant seasonal asymmetries and differences between

hot and cold shocks, though the patterns point to distinct underlying mechanisms. In the immediate aftermath of temperature shocks (horizon h=0), we observe that hot shocks during fall, winter and spring already yield negative point estimates, albeit not statistically significant. Suggesting early signs of deflationary pressure. In contrast, cold shocks tend to exert upward pressure on energy prices on impact, particularly in fall and winter, where point estimates are positive.For warm winters, the initially small decline in impact becomes increasingly pronounced and statistically significant at horizons one to three, as shown in Table 5. The effect reaches –0.64 at horizon one and peaks at –0.88 at horizon two, remaining significant at –0.87 at horizon three. In the short-term, the picture is similar for hot falls, as the point estimates for horizon two and three increase in magnitude and turn significant as well. Both results support the interpretation that unexpectedly mild winters (or falls) substantially reduce heating needs and energy consumption, causing energy price to decrease. One of the main channels in the work of Lucidi et al. (2024). For hot spring periods, we find a similar pattern, since two and three months after the shock the negative response is largest in magnitude and statistically significant. The explanation of lower energy demand might apply here as well. However, an additional mechanism may help explain these patterns more fully: the role of renewable energy production. In 2023, Germany had the highest share of solar and wind in electricity production among European countries (39.88%), according to data from the International Energy Agency. Wind energy is more prevalent in fall and winter, while solar dominates during the warmer months. Thus, warmer fall and winter periods—with higher solar radiation—may lead to increased renewable energy supply, amplifying the deflationary effect of reduced demand. Conversely, colder and likely cloudier periods reduce renewable output, reinforcing the upward price pressure from increased heating demand. On top of that, warmer spring and summer periods (with more sun hours) lead to even more flexible production conditions. Supporting this interpretation, summer shocks indicate no significant effects in the short run. Estimates fluctuate around

zero, suggesting that increased cooling demand may be offset by higher renewable supply.

With respect to cold shocks and reaction of energy prices, the results are much more mixed and less meaningful. The largest (though still statistically insignificant) estimate among cold shocks is observed for winter periods. However, such an effect does not persist even in the periods immediately after the shock. There might be a short lived upward pressure on prices from increased heating demand, but seems to be limited at best. Cold shocks in fall show gradually increasing point estimates, from 0.19 at impact to 0.47 at horizon 1. Although not statistically significant, the trend is consistent with rising heating needs ahead of winter. For spring and summer estimates fluctuate around zero with no significant changes. We would argue that there is no measurable price effect in the short run, possibly due to low heating needs and more flexible supply in those seasons, as already mentioned.

Table 5: Effects on Impact for Energy Prices

	Energy Inflation			
	Horizon 0	Horizon 1	Horizon 2	Horizon 3
Hot Winter	-0.18	-0.64**	-0.88**	-0.87*
	(0.19)	(0.27)	(0.43)	(0.44)
Hot Spring	-0.37	-0.30	-0.67*	-1.04**
	(0.24)	(0.35)	(0.35)	(0.44)
Hot Summer	0.15	-0.13	0.28	-0.51
	(0.15)	(0.31)	(0.38)	(0.41)
Hot Fall	-0.12	-0.06	-0.57*	-0.59*
	(0.17)	(0.22)	(0.29)	(0.31)
Cold Winter	0.28	0.33	-0.07	-0.25
	(0.19)	(0.28)	(0.34)	(0.47)
Cold Spring	-0.17	0.06	0.04	0.00
	(0.15)	(0.27)	(0.39)	(0.40)
Cold Summer	0.18	-0.17	0.16	-0.18
	(0.22)	0.47)	(0.45)	(0.63)
Cold Fall	0.19	0.47	0.30	0.10
	(0.24)	(0.34)	(0.45)	(0.55)
Time Trends	Yes	Yes	Yes	Yes
Observations	288	287	286	285
R^2	0.45	0.43	0.45	0.46

Newey-West standard errors in parentheses

* $p < 0.10$, ** $p < 0.05$, *** $p < 0.01$

In the medium term, the impulse response functions in figure 6 offer additional insights

into the dynamics of energy price adjustments. Several patterns observed in the short term persist or even intensify, while others fade, suggesting that the transmission of temperature shocks to energy prices is not uniform across seasons or shock types. For hot temperature shocks, the most pronounced and persistent effect is again observed in winter. Energy prices show a marked and statistically significant decline over several months after the shock, before turning back to the pre-shock level after approximately 12 months. This corroborates the earlier finding of lower heating needs and improved supply conditions due to unexpectedly mild winter conditions, which continue to dampen prices well beyond the immediate period. A similar finding is made by Lucidi et al. (2024). The pattern is also visible in fall, where energy inflation remains below baseline for up to five months after the shock, though the effect is smaller in magnitude. For hot spring periods the response for the first five month is almost identical. However, after roughly 12 months it becomes significantly positive, that reaction remaining persistent for multiple periods. This result seems to somewhat counter intuitive. For summer shocks, impulse responses are more volatile and less conclusive. While there is tendency of downward movement, especially 12-20 months after the shock, consistent with the earlier interpretation of more flexibility in energy production during these months. That being said, the results regarding spring and summer require closer examination. While the immediate impact for hot springs is driven by reduced heating needs and favorable solar supply, wholesale prices fall, and there is a pass-through to lower consumer prices as well. However, as the sun's intensity during spring is lower compared to summer, energy supply based on solar production in the summer is comparably larger. Moreover, given the assumption that during warm spring days the demand for cooling devices might increase, the relative increase of demand outweighs the relative increase of supply in the spring leading to higher (delayed) energy prices in the spring but not in the summer, where the relative increase of supply might outweighs the relative increase of energy demand.

As before cold shocks exhibit less pronounced effects. Although cold shocks in fall and

winter initially show some upward price pressure, these effects largely dissipate after a few months. The impulse responses quickly return to baseline, and confidence bands generally include zero throughout the forecast horizon. The fall is an exception, as energy prices persistently increase by up to 1 percentage point 10 months later, then turning back to the initial level. However, overall such shocks do not translate into sustained energy-inflationary dynamics. Interestingly, while observed an persistent increase after 12 months for hot spring, we see the opposite for cold springs. After an initial increase in energy use (due to cold spring months), markets may adjust by building up reserves or expanding supply, which can result in oversupply and downward pressure on prices in the medium term. Additionally, behavioral adjustments could further contribute to a delayed deflationary response. Responses after summer shocks continue to show no clear pattern, while tending to be deflationary, but with wide confidence bands. Nevertheless, this again supports the interpretation that demand effects are limited outside the heating season and that supply-side adjustments may help cushion potential price impacts. Taken together, the medium-term responses reinforce the notion that hot shocks — particularly during heating-intensive seasons — have more persistent and pronounced effects on energy inflation than cold shocks.

5.2.3 Inflation

Finally, we assess the implications of cold and hot temperature shocks on the German headline consumer price index. Consistent with what we find for the disaggregated prices, we again observe an asymmetric as well as heterogeneous impact of the idiosyncratic cold and hot weather shocks on the German consumer price index. What stands out most is that headline inflation following a temperature shock—whether hot or cold—is primarily driven by changes in energy prices. This is most clearly illustrated by the example of warm winters: for warm winter (or fall) periods, we observe persistent (transitory) deflationary effects on the Consumer Price Index (CPI), closely mirroring the response of the energy component. When excluding only the energy component from headline inflation (see third row in

Figure 6: Impulse response functions for the energy component of the harmonized index of consumer prices, shown separately for hot temperature shocks (red) and cold temperature shocks (blue), presented for each calendar season. The respective shaded areas represent 68% confidence intervals computed using Newey–West standard errors.

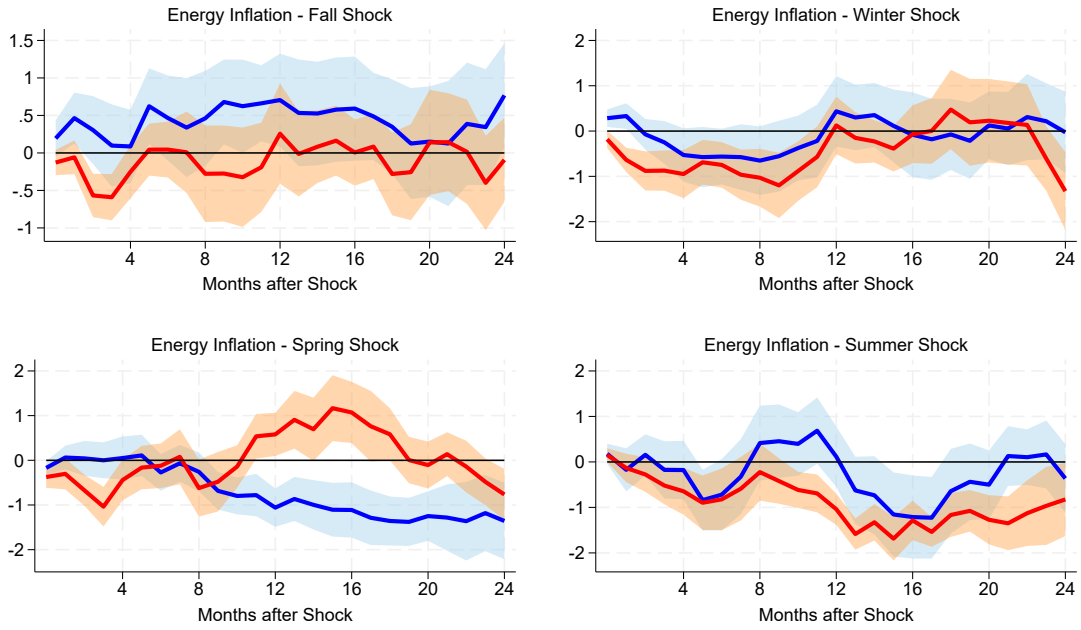

Figure 7), the previously significant short- and medium-term effects of a hot temperature shock on the CPI during winter and fall disappear. In spring, we observe an asymmetric response: cold (hot) temperature shocks decrease (increase) the German CPI with a lag of approximately 12 months. This asymmetry appears to be mainly driven by the energy price response—specifically, a drop in energy prices after cold spring periods, and increased prices due to higher cooling demand following warm spring periods (compare the first plot in the second row of Figure 6 with the third plots in the first and second rows of Figure 7). When energy is excluded, this asymmetric response disappears (see third plot in the third row of Figure 7). Further supporting this interpretation, Figure 7, row two, shows the impulse responses of the CPI when only food is excluded. The trajectories remain virtually identical to those of headline inflation, again pointing to the central role of energy prices. When both food and energy are excluded (i.e., core inflation), the responses differ markedly from those

of headline inflation.

Taken together, this evidence suggests that temperature shocks mainly transmit to the German CPI through their impact on energy prices, while the effect on food prices is largely confined to that sector. Energy prices play a particularly prominent role, as energy serves as a crucial input factor across nearly all areas of the economy. Supporting this notion, producer prices for energy also rise following temperature shocks (see appendix). In contrast, food prices seem to exert a much smaller influence on headline inflation in a high-income country like Germany, likely due to their relatively low weight in the general consumption basket. This interpretation aligns with findings from studies covering broader country samples—such as Kotz et al. (2024) and Faccia et al. (2021)—which show food prices to be a major driver of inflation in lower-income economies. An additional interesting case is the summer period: when both food and energy prices are controlled for, we observe a lagged inflationary effect around five months after the shock, regardless of whether the summer was unusually hot or cold. This effect may be linked to service inflation; however, results in this regard remain inconclusive.

5.3 Sensitivity Analysis

In this section, we perform a comprehensive series of additional tests to pin down the underlying mechanisms of our results. Specifically, we try to distinguish between demand and supply side effects by conducting additional analysis on production indices and consumption values. On top of that, we examine the robustness of our main results with respect to nonlinear impacts and interaction with different weather events. Further checks (regarding learning horizon, aggregation weighting or comparison with other measures), along with all relevant tables and figures, are provided in appendix 7.13.

Figure 7: Impulse response functions for the energy component of the harmonized index of consumer prices, shown separately for hot temperature shocks (red) and cold temperature shocks (blue), presented for each calendar season. The respective shaded areas represent 68% confidence intervals computed using Newey–West standard errors.

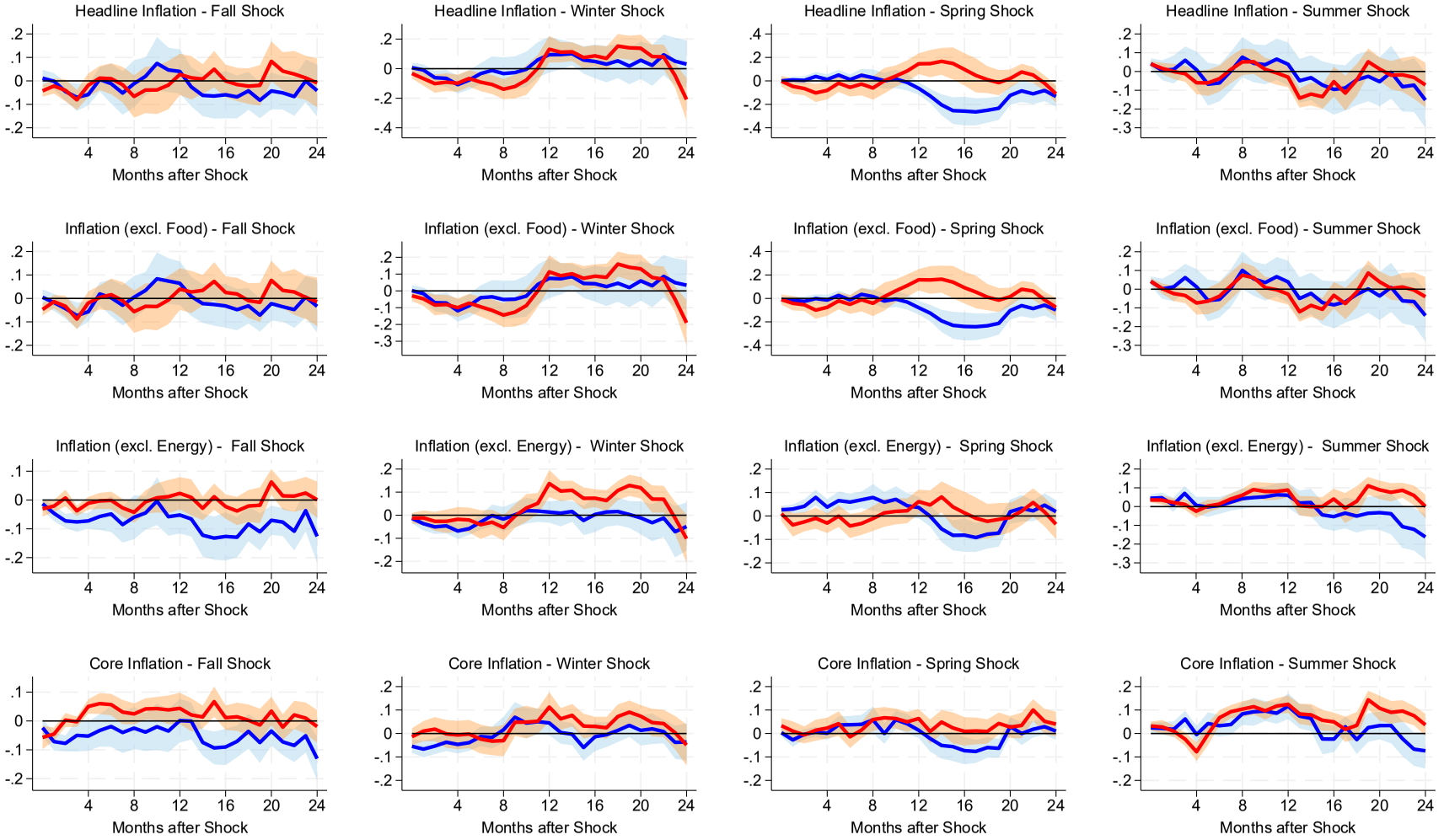

5.3.1 Demand vs. Supply Effects

To better understand whether supply disruptions (or pushes) or demand adjustments cause our price movements (Ciccarelli and Marotta (2024)), we estimate a very similar model as in equation 10, but now using two different production indices as dependent variables: total industrial production and energy production. By doing that we follow Lucidi et al. (2024). As our primary interest lies in understanding the overall effect of weather shocks rather than their dynamic trajectory, we focus on and report only the contemporaneous impact (h = 0) in table 6. This allows for a more straightforward interpretation of the immediate effects, abstracting from potential lagged responses. Another adjustment compared to model 10 is that we merge spring and summer into a single "warmer" season, and fall and winter into a "colder" season. We then interact our shock series' with the respective season dummies, as in the previous specification. In addition, we draw on data from the Agorameter database on Germany's electricity mix. The dataset provides monthly supply quantities by production type—solar, onshore wind, total renewables, and the aggregate for conventional energy production—from 2012 onwards. Although the sample period is relatively short, it offers valuable insights into the underlying mechanisms.

Hot springs and summers significantly reduce total industrial production by 0.27 percentage points, likely reflecting the vulnerability of sectors exposed to outdoor conditions and physical labor. In contrast, the energy sector responds positively (0.17) during these periods. Two potential mechanisms may explain this effect: (1) an increase in supply driven by higher solar energy production, and (2) elevated electricity demand for cooling. However, as shown previously, energy prices tend to decline in summer months—regardless of whether shocks are heat- or cold-related—providing stronger support for the supply-side explanation via expanded solar output. Supporting this, solar production increases significantly by 1.15 percentage points, indicating improved supply conditions. Nevertheless, the total value of renewables does not rise significantly, likely due to a muted or offsetting response from wind

energy.

Table 6: Effects on Impact - Production and Energy Supply

	IP	IP-Energy	Solar	Wind (onshore)	Renewables Total	Conventional Total
Hot Spring + Summer	-0.27*	0.17	1.15***	0.01	-0.03	0.33
	(0.15)	(0.20)	(0.36)	(0.70)	(0.25)	(0.20)
Hot Fall + Winter	0.13	-0.81***	1.67***	0.90	0.74**	-0.44**
	(0.11)	(0.20)	(0.74)	(0.76)	(0.35)	(0.17)
Cold Spring + Summer	-0.15	0.77***	0.21	1.82**	0.38	0.19
	(0.19)	(0.21)	(0.50)	(0.80)	(0.31)	(0.17)
Cold Fall + Winter	-0.32*	0.57***	0.57	-2.24**	-1.01**	0.47**
	(0.16)	(0.22)	(1.01)	(1.07)	(0.47)	(0.23)
Add. Control Variables	Yes	Yes	No	No	No	No
Time Trends	Yes	Yes	Yes	Yes	Yes	Yes
Observations	299	299	95	95	95	95
R^2	0.28	0.35	0.59	0.42	0.50	0.61

Newey-West standard errors in parentheses

* $p < 0.10$, ** $p < 0.05$, *** $p < 0.01$

Hot winters, while exerting no significant effect on overall industrial production, cause a pronounced and significant drop in energy production (-0.81 percentage points), consistent with reduced heating demand and the observed weakening of winter energy prices. Concurrently, we observe significant increases in solar and total renewables production (and an insignificant rise in wind), further explaining the previously documented decline in energy prices. However, a trade-off appears to exist between renewable and conventional energy sources, as conventional output declines significantly.

Conversely, cold shocks lead to significant increases in energy production across both seasonal groupings, with a stronger effect during spring and summer (0.77 percentage points) compared to fall and winter (0.57 percentage points). This pattern likely reflects heightened energy demand due to low temperatures. On the supply side, two notable patterns emerge: wind energy increases significantly during cold springs and summers, but decreases (along with renewables overall) during fall and winter. In the latter period, conventional production appears to compensate by increasing, thus explaining the overall rise in energy production, caused by rising demand. The heterogeneous response of wind energy across seasons may be

attributed to underlying meteorological and technical factors. Wind patterns in Germany typically exhibit stronger and more consistent speeds during the fall and winter months, yet adverse conditions such as ice accumulation and cold temperatures can impair turbine efficiency, potentially explaining the observed decline in wind production during cold fall and winter periods. Conversely, cold shocks in spring and summer may coincide with favorable wind conditions, leading to a significant increase in wind energy output.

In the energy sector, the consistent co-movement of production and prices across temperature shocks—i.e., higher prices and higher output during cold spells, and lower prices with reduced output during warm winters—suggests that demand-side dynamics also play a key role. Increased heating or cooling needs appear to drive both higher prices and increased production. To further support this claim, we also look at consumption quantities. Specifically, consumption in gas and electricity. Unlike the previous analysis, this approach does not rely on seasonal breakdowns but instead uses heating degree days (HDD) and cooling degree days (CDD) as proxies for temperature-related energy needs. Again, we follow Lucidi et al. (2024) and construct dummy variables indicating whether the number of HDDs or CDDs in a given year has increased or decreased compared to the previous year—reflecting warmer or colder conditions, respectively. These dummies are then interacted with the corresponding heat shock. We opted for this strategy, as climate change in general lead to higher average temperatures. For example, when HDDs fall and/or CDDs rise—indicating milder/warmer temperature levels—a heat shock is expected to further reduce heating needs, thereby lowering gas demand. At the same time, higher CDDs may suggest increased cooling needs, so a heat shock under these conditions may lead to a rise in electricity demand.

Table 7 shows the results. The interaction between a heat shock and a decline in HDDs (i.e., a warmer month compared to last year) shows a strong and statistically significant drop in gas consumption (-7.43 percentage points), accompanied by a smaller albeit insignificant reduction in electricity use (-0.46). This aligns with the interpretation that warmer-than-

Table 7: Effects on Impact - Energy Demand

	Gas Consumption	Electricity Consumption
Heat shock $\times \text{HDD}_{\text{negative}}$	-7.43***	-0.46
	(2.49)	(0.66)
Heat shock $\times \text{CDD}_{\text{positive}}$	0.04	0.77
	(3.03)	(0.75)
Time Trends	Yes	Yes
Observations	143	143
R^2	0.70	0.81

Newey-West standard errors in parentheses
* $p < 0.10$, ** $p < 0.05$, *** $p < 0.01$

usual months reduce heating needs, and thus lower energy demand—consistent with the earlier finding of reduced energy production during hot winters. The interaction between a heat shock and increased CDDs (indicating e.g. a hotter summer) does not affect both gas and electricity demand significantly. However, estimates have a positive sign. This suggests that while hotter summers may increase cooling needs, the effect on energy consumption is modest particularly in relatively mild country like Germany. Lucidi et al. (2024) find the same for European countries, arguing that a "turn-off-heating effect" outweighs a so-called "turn-on-cooling" effect. Overall, these findings mirror the earlier production results, where energy output rose modestly during summers—likely driven by increased supply (e.g., solar) rather than strong demand pressure.

Taken together, the sectoral asymmetries in price–quantity relationships support the interpretation that demand effects dominate in the energy sector, with heating demand (particularly for gas) responding strongly to both cold and warm conditions. These demand effects are accompanied and reinforced by shifts in the relative importance of energy sources: under favorable conditions, renewable energy production expands, further contributing to downward pressure on energy prices.

5.3.2 Nonlinearities

Burke and Miguel (2015) have demonstrated that even high-income economies respond in a highly non-linear way to local temperature shocks. Hence, in this section, we account

for additional nonlinear effects[20] of temperatures on agricultural production and energy demand. The underlying idea is that, for example, 1–2 hot days may have minimal effects on agriculture and food prices, whereas 8–9 or more days within a month can have a significantly larger negative (or positive) impact. The same argument can be applied to cold days and energy demand. To capture such mechanisms in our econometric framework, we created various indicator variables. The first indicator takes the value of one if the number of hot days falls between 0 and 4.99, and zero otherwise. The second becomes 1 for the interval $5 - 9.99$, and the final indicator becomes one for all cases exceeding 10 hot days. Doing the same for cold days, we end up with six dummy variables, which we include in our local projection estimation from above instead of our shocks[21]. The corresponding IRFs are presented in Figure 8, focusing solely on food and energy prices due to their central relevance in our main findings. The first row covers the responses to hot temperature shocks, while row two covers cold ones. Qualitatively, the results do not change compared to our previous findings. Nevertheless, we see some interesting patterns emerging. Food prices do not increase following a month with a relatively small hot temperature shock ($0\breve{}4.99$ days). However, for larger numbers of hot days, we observe a significant rise in prices, with the magnitude of the response increasing as the number of hot days grows (Compare the dark red line in the first plot of figure 8 with the red-orange line in the same plot.). Once again, an S-shaped reaction is evident, with prices returning to their original levels roughly five months after the shock. For months with more than 10 hot days, prices even decrease eight months later, and this decline persists throughout the observed horizon, probably due to demand effects. The size of the impact (up to two percentage points) is even bigger compared to our baseline result for food prices. Interestingly, regarding cold spells, the biggest response

[20]The inclusion of seasonal dependencies has already demonstrated the presence of highly nonlinear relationships.

[21]Here, we do not take into account seasonal influences.

Figure 8: Impulse response functions for the energy and food components of the harmonized index of consumer prices, displayed for different intervals (dummy variables) based on the number of hot or cold days. The respective shaded areas represent 68% confidence intervals computed using Newey–West standard errors.

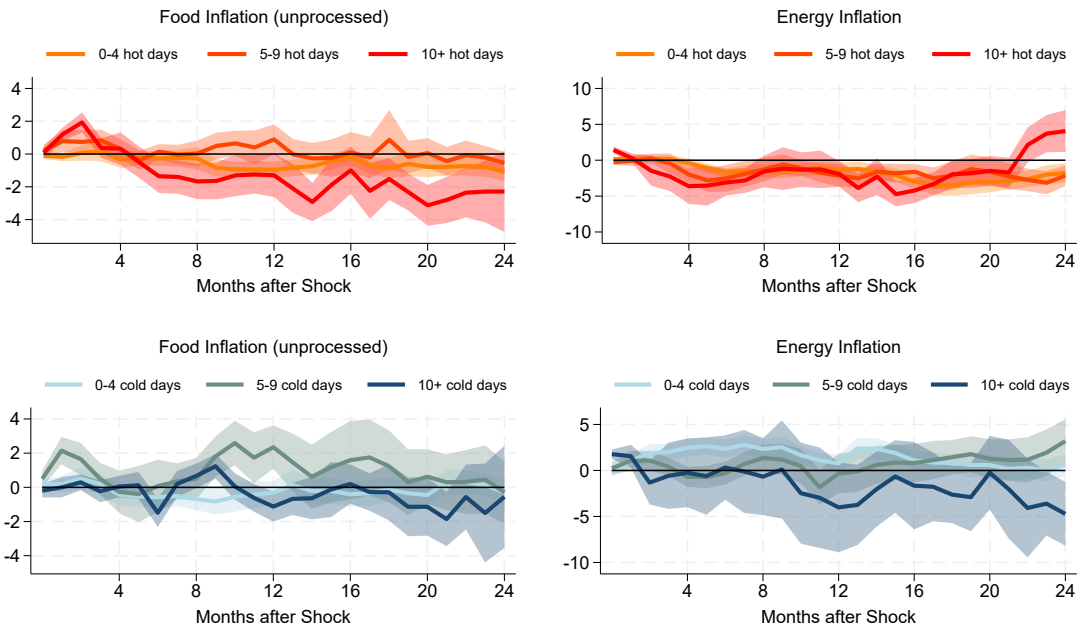

(in magnitude and significance) follows after a medium ($5 - 9.99$ days) shock, with a sharp increase of almost 2 percent three months after the shock. For other intervals, we cannot see such behavior. Once again, for food prices, we see the S-shaped type behavior, where price returns back to the pre-shock level after a couple of months. However, it comes a bit by surprise that severe cold shocks do not have any impact here (first plot, second row of figure 8). Turning to energy prices, IRFs are almost identical as in figure 6. Even for a small number of hot days, prices begin to decline around six months after the shock. For the other two intervals, the decrease starts almost immediately, reaching a reduction of up to 5 percent. This decline remains both significant and substantial in magnitude throughout the entire horizon. The same was found for the effect of warm (winter) shocks in our baseline specifications. Also, with respect to cold shocks,, the responses are as expected with increasing prices for all intervals. The largest rise by approximately four percent is caused

by the largest number (10+) of cold days; also for $5 - 9.99$ days, the reaction is relevant. However, the price increases and finally returns back to the original level. In conclusion, the responses shown in Figure 8 provide clear evidence of the existence and relevance of nonlinear relationships concerning shock size. Generally, the largest shock values trigger the most significant responses, while short occurrences of extremes appear to cause minimal impact. Nevertheless, the results support our previous findings and, therefore provide a certain robustness.

5.3.3 Growing Season

As argued by Harari and Ferrara (2018), during the growing season crops are sensitive to unfavorable weather conditions, which might—and thus should—affect food supply. Therefore, we examine the effects of temperature shocks during the crop growing season. For this, we utilize aggregated data for Germany from the Climate Change Knowledge Portal by the World Bank, which provides the start and end dates of the yearly growing season. In general, the start of the growing season is defined as the day of the year that reflects the first span of at least 6 consecutive days with a daily mean temperature above 5 °C. Based on this information, we create a dummy variable indicating whether a month falls within the growing season or not. On average, it lasts from March until November. This dummy is then interacted with our weather shocks to capture the effects. Thus, we are estimating a similar regression as in equation 10 but with growing and not calendar seasons. Further, we include sun duration and precipitation per month as additional controls.[22] The corresponding IRFs are shown in Figure 9, focusing on the different food components (processed, non-processed, and overall) of the HICP, as well as a self-constructed index that includes all items except food. The emphasis on food is intuitive, as growing seasons are likely to affect agricultural production and, consequently, food prices most. When compared to previous results, we still

[22] Aggregated data is taken from the Deutscher Wetterdienst.

Figure 9: Impulse response functions for the food components of the harmonized index of consumer prices, shown separately for hot temperature shocks (red) and cold temperature shocks (blue) during crop growing season. The respective shaded areas represent 68% confidence intervals computed using Newey–West standard errors.

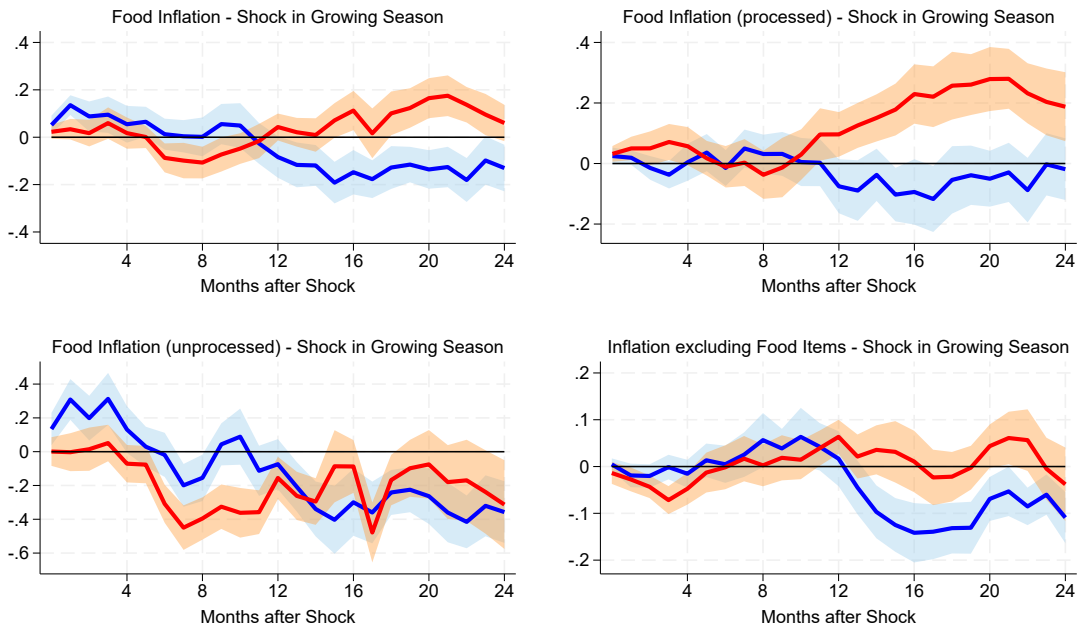

observe the characteristic S-shaped pattern: food prices initially increase on impact, then decrease, and sometimes even turn negative. However, this behavior is more pronounced for cold temperature shocks during the growing season and is less evident—or even absent—for hot shocks, which is somewhat surprising. A possible explanation is that as the growing season in Germany typically spans March to November, encompassing spring, summer, and fall. As such, the impacts during spring and fall (where according to figure 5 prices decrease) may overshadow those from summer. From this, we conclude that in Germany, with its relatively moderate climate, particularly hot temperature shocks only impact food prices when they occur during summer, a period characterized by high absolute temperatures. This finding is completely in line with that from Faccia et al. (2021), which also quantified such an effect for summer. However, we demonstrate that this mechanism is also at play in an economically advanced country like Germany. As a last note, the typical S-shape is specific to food prices;

no comparable response is observed when excluding the food component (see the second plot in the second row of Figure 9).

5.3.4 Droughts

Beyond temperature fluctuations, precipitation levels - or lack thereof - represent a critical factor influencing agricultural output and food prices. In this section, we investigate the effects of drought conditions in conjunction with temperature shocks as part of an additional robustness analysis. To this end, we utilized aggregated precipitation data for Germany obtained from the Deutscher Wetterdienst (DWD) and constructed a drought indicator variable based on the Standardized Precipitation Index (SPI) at a monthly resolution. If the SPI falls below -1, our dry dummy takes the value of one, and zero otherwise. Following previous studies such as Felbermayr and Gröschl (2014) and Bodenstein and Scaramucci (2025), which define a drought as at least two consecutive months of unusually low precipitation, we construct a final drought dummy equal to one when the dry dummy is equal to one for two consecutive months. Figure 10 illustrates a negative correlation between the SPI and the occurrence of hot temperature shocks, but this relationship is evident only during the spring and summer months. Concurrently, the correlation coefficient between the drought dummy variable and the temperature shock is significantly positive, again limited to the spring and summer periods. In contrast, when examining the full year or restricting the analysis to the fall and winter months, these correlations are no longer observed. Given the pronounced dependence of agricultural production on conditions during the warmer seasons, the subsequent analysis concentrates on extreme weather events occurring specifically in spring and summer. Accordingly, we replicate the estimation specified in equation 10, differentiating only between the spring–summer and fall–winter periods, and allowing the drought dummy to interact with the heat-related temperature shock.[23] As anticipated, food prices rise sig-

[23] Both types of temperature shocks (hot and cold) are included in the model; however, the figure displays only the effects of the heat shock.

Figure 10: Correlation between heat shock and SPI for spring-summer periods vs fall-winter periods.

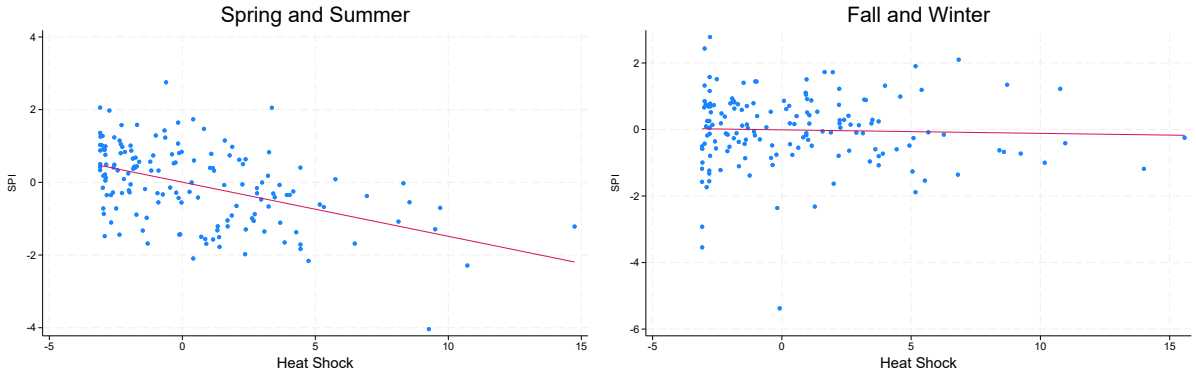

nificantly following hot and dry periods, with increases of up to 0.5 percent. Approximately six months after the shock, prices revert to their pre-shock levels, exhibiting an S-shaped adjustment pattern similar to that observed in our main results. In contrast, for non-food items, no significant price response is detected.

Figure 11: Impulse response functions for the (unprocessed) food component of the harmonized index of consumer prices, versus the index excluding unprocessed food items. The graph only features the heat shock. The respective shaded areas represent 68% confidence intervals computed using Newey–West standard errors.

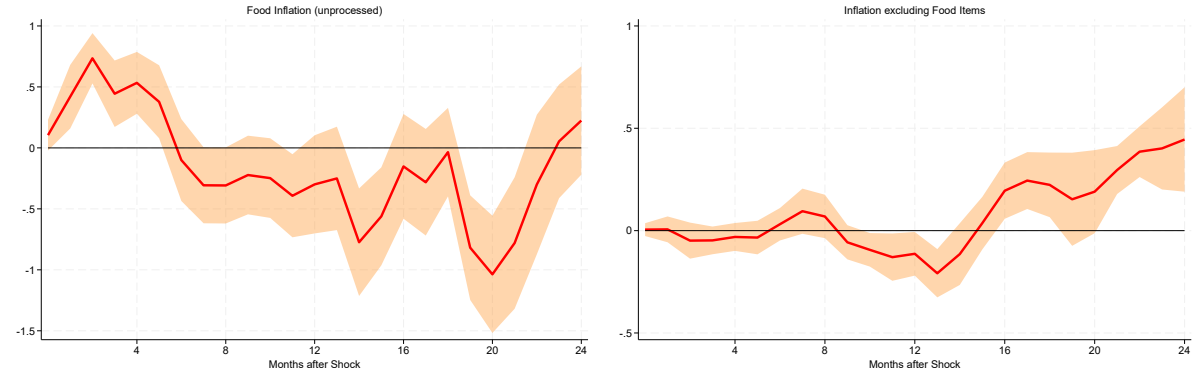

We also incorporated extreme-precipitation (heavy rainfall) events, but this dimension did not yield clear or robust results; we therefore do not consider these events further in our analysis. One plausible explanation for the significant effects we find for drought—relative

to heavy rain—is that drought is typically a regional to subcontinental and persistent phenomenon, driven by large-scale circulation anomalies and land–atmosphere feedbacks, with durations commonly spanning weeks to seasons (and sometimes years). By contrast, heavy-precipitation events are usually mesoscale and short-lived (hours to a few days) and thus more localized; hence, their effects on food-price inflation are unclear.

6 Conclusion

Our analysis demonstrates that extreme temperature shocks—both hot and cold—have measurable and economically significant effects on price dynamics in Germany. The impact is concentrated in food and energy markets, which not only play a central role in shaping headline inflation but are themselves highly sensitive to climate-related disruptions. The evidence points to distinct transmission mechanisms: food prices react mainly through supply-side constraints, particularly via agricultural productivity losses, while energy prices respond predominantly through shifts in demand for heating and cooling. In both cases, these sectoral effects translate into noticeable movements in the overall price level.

Our contribution to the literature is threefold. First, we document the heterogeneous effects of hot and cold extremes, extending the focus beyond the positive temperature deviations emphasized in prior work. Cold spells often generate opposite price dynamics to heat extremes, particularly for food and energy. Second, we show strong seasonal nonlinearities: in winter and spring, warmer weather dampens food prices while cold spells raise them; in summer, heat extremes sharply increase food prices before they return to pre-shock levels, likely reflecting harvest damage. Energy prices are especially sensitive in winter, with cold spells driving prices up through higher demand and reduced renewable generation, while mild winters lead to significant declines. Third, these sectoral responses reveal that headline inflation in Germany is primarily driven by energy price movements—consistent with the 2022 episode, when surging energy costs spilled over to nearly all sectors. Beyond seasonality, larger shock magnitudes amplify price responses, and our results remain robust when

accounting for renewable energy production, droughts, and crop cycles.

Methodologically, our shock design allows us to separate hot from cold extremes. This refinement reduces the risk of overlooking regional weather phenomena during aggregation and prevents extremes from being averaged out over time, enabling a clearer identification of asymmetric effects. While our analysis focuses on Germany, the approach can be readily adapted to a euro area panel to study cross-country heterogeneity and potential inflation spillovers—an issue of clear relevance for monetary policy in an integrated market. Beyond inflation, the shock measure could also be applied to study other climate-sensitive economic outcomes, such as health impacts affecting labor productivity or interactions with other macroeconomic shocks, which remain important avenues for future research.

7 Bibliography

Acevedo, S., Mrkaic, M., Novta, N., Pugacheva, E., and Topalova, P. (2020). The effects of weather shocks on economic activity: What are the channels of impact? *Journal of Macroeconomics*, 65:103207.

Angrist, J. D. and Pischke, J.-S. (2009). *Mostly harmless econometrics: An empiricist's companion*. Princeton university press.

Auffhammer, M., Hsiang, S. M., Schlenker, W., and Sobel, A. (2013). Using weather data and climate model output in economic analyses of climate change. *Review of Environmental Economics and Policy*.

Auffhammer, M. and Mansur, E. T. (2014). Measuring climatic impacts on energy consumption: A review of the empirical literature. *Energy Economics*, 46:522–530.

Auffhammer, M. and Schlenker, W. (2014). Empirical studies on agricultural impacts and adaptation. *Energy Economics*, 46:555–561.

Benchimol, J. and Bounader, L. (2023). Optimal monetary policy under bounded rationality. *Journal of Financial Stability*, 67:101151.

Berg, K. A., Curtis, C. C., and Mark, N. C. (2024). Gdp and temperature: Evidence on cross-country response heterogeneity. *European Economic Review*, 169:104833.

Bilal, A. and Känzig, D. R. (2024). The macroeconomic impact of climate change: Global vs. local temperature. Technical report, National Bureau of Economic Research.

Bodenstein, M., Erceg, C. J., and Guerrieri, L. (2011). Oil shocks and external adjustment. *Journal of International Economics*, 83(2):168–184.

Bodenstein, M. and Scaramucci, M. (2025). On the gdp effects of severe physical hazards. *European Economic Review*, page 105019.

Bordalo, P., Gennaioli, N., Ma, Y., and Shleifer, A. (2020). Overreaction in macroeconomic expectations. *American Economic Review*, 110(9):2748–82.

Burke, M., H. S. and Miguel, E. (2015). Global non-linear effect of temperature on economic production. *Nature*, 527:235–239.

Burke, M., González, F., Baylis, P., Heft-Neal, S., Baysan, C., Basu, S., and Hsiang, S. (2018). Higher temperatures increase suicide rates in the united states and mexico. *Nature climate change*, 8(8):723–729.

Burke, M., Hsiang, S. M., and Miguel, E. (2015). Global non-linear effect of temperature on economic production. *Nature*, 527(7577):235–239.

Carleton, T. A. and Hsiang, S. M. (2016). Social and economic impacts of climate. *Science*, 353(6304):aad9837.

Chafwehé, B., Colciago, A., and Priftis, R. (2025). Reallocation, productivity, and monetary policy in an energy crisis. *European Economic Review*, 173:104963.

Choi, D., Gao, Z., and Jiang, W. (2020). Attention to global warming. *The Review of Financial Studies*, 33(3):1112–1145.

Ciccarelli, M., Kuik, F., and Hernández, C. M. (2023). The asymmetric effects of weather shocks on euro area inflation.

Ciccarelli, M. and Marotta, F. (2024). Demand or supply? an empirical exploration of the effects of climate change on the macroeconomy. *Energy Economics*, 129:107163.

Coibion, O. and Gorodnichenko, Y. (2015). Information rigidity and the expectations formation process: A simple framework and new facts. *American Economic Review*, 105(8):2644–78.

Coumou, E., Capua, G. D., Vavrus, S., Wang, L., and Wang, S. (2018). The influence of arctic amplification on mid-latitude summer circulation. *Nature Communication*, page 2959.

Crofils, C., Gallic, E., and Vermandel, G. (2025). The dynamic effects of weather shocks on agricultural production. *Journal of Environmental Economics and Management*, 130:103078.

Dasgupta, S., Van Maanen, N., Gosling, S. N., Piontek, F., Otto, C., and Schleussner, C.-F. (2021). Effects of climate change on combined labour productivity and supply: an empirical, multi-model study. *The Lancet Planetary Health*, 5(7):e455–e465.

Dell, M., Jones, B. F., and Olken, B. A. (2012). Temperature shocks and economic growth: Evidence from the last half century. *American Economic Journal: Macroeconomics*, 4(3):66–95.

Dell, M., Jones, B. F., and Olken, B. A. (2014). What do we learn from the weather? the new climate-economy literature. *Journal of Economic literature*, 52(3):740–798.

Deryugina, T. (2013). How do people update? the effects of local weather fluctuations on beliefs about global warming. *Climatic change*, 118:397–416.

Deschênes, O. and Greenstone, M. (2011). Climate change, mortality, and adaptation: Evidence from annual fluctuations in weather in the us. *American Economic Journal: Applied Economics*, 3(4):152–185.

Donadelli, M., Jüppner, M., Riedel, M., and Schlag, C. (2017). Temperature shocks and welfare costs. *Journal of Economic Dynamics and Control*, 82:331–355.

Drudi, F., Moench, E., Holthausen, C., Weber, P.-F., Ferrucci, G., Setzer, R., Nino, V. D., Barbiero, F., Faccia, D., Breitenfellner, A., et al. (2021). Climate change and monetary policy in the euro area. *ECB Occasional Paper Series No 271*.

ECB (2024). Economic, financial and monetary developments. *ECB Economic Bulletin, Issue 2/2024*.

Faccia, D., Parker, M., and Stracca, L. (2021). Feeling the heat: extreme temperatures and price stability.

Felbermayr, G. and Gröschl, J. (2014). Naturally negative: The growth effects of natural disasters. *Journal of development economics*, 111:92–106.

Gabaix, X. (2020). A behavioral new keynesian model. *American Economic Review*, 110(8):2271–2327.

Gali, J. (2015). *Monetary Policy, Inflation, and the Business Cycle: An Introduction to the New Keynesian Framework and Its Applications - Second Edition*. Princeton University Press.

Harari, M. and Ferrara, E. (2018). Conflict, climate, and cells: A disaggregated analysis. *The Review of Economics and Statistics*, 100(4):594–608.

Hatfield, J. L. and Prueger, J. H. (2015). Temperature extremes: Effect on plant growth and development. *Weather and climate extremes*, 10:4–10.

Hersbach, H., Bell, B., Berrisford, P., Hirahara, S., Horányi, A., Muñoz-Sabater, J., Nicolas, J., Peubey, C., Radu, R., Schepers, D., et al. (2020). The era5 global reanalysis. *Quarterly Journal of the Royal Meteorological Society*, 146(730):1999–2049.

Hsiang, S. (2016). Climate econometrics. *Annual Review of Resource Economics*, 8(1):43–75.

Hsiang, S. M., Burke, M., and Miguel, E. (2013). Quantifying the influence of climate on human conflict. *Science*, 341(6151):1235367.

Jordà, Ò. (2005). Estimation and inference of impulse responses by local projections. *American economic review*, 95(1):161–182.

Kim, H. S., Matthes, C., and Phan, T. (2022). Severe weather and the macroeconomy. *Federal Reserve Bank of Richmond Working Papers, 21-14R*.

Kohlhas, A. N. and Walther, A. (2021). Asymmetric attention. *American Economic Review*, 111(9):2879–2925.

Kotz, M., Kuik, F., Lis, E., and Nickel, C. (2024). Global warming and heat extremes to enhance inflationary pressures. *Communications Earth & Environment*, 5(1):116.

Lucidi, F. S., Pisa, M. M., and Tancioni, M. (2024). The effects of temperature shocks on energy prices and inflation in the euro area. *European Economic Review*, 166:104771.

Meggiorini, G. (2023). Behavioral new keynesian models: An empirical assessment. *Journal of Macroeconomics*, 77:103538.

Moore, F. C. and Lobell, D. B. (2015). The fingerprint of climate trends on european crop yields. *Proceedings of the National Academy of sciences*, 112(9):2670–2675.

Natoli, F. (2023). The macroeconomic effects of temperature surprise shocks. *Bank of Italy Temi di Discussione (Working Paper) No*, 1407.

Papageorgiou, C., Saam, M., and Schulte, P. (2017). Substitution between clean and dirty energy inputs: A macroeconomic perspective. *The Review of Economics and Statistics*, 99(2):281–290.

Parker, M. (2018). The impact of disasters on inflation. *Economics of Disasters and Climate Change*, 2(1):21–48.

Pataracchia, B., Pfeiffer, P., Ratto, M., and Teresinski, J. (2023). Energy prices as drivers of inflation and real output: An estimated structural model for the euro area. Technical report, Tech. rep., unpublished manuscript.

Portillo, R., Zanna, L.-F., O'Connell, S., and Peck, R. (2016). Implications of food subsistence for monetary policy and inflation. *Oxford Economic Papers*, 68(3):782–810.

Ramey, V. A. (2016). Macroeconomic shocks and their propagation. *Handbook of macroeconomics*, 2:71–162.

Rousi, E., Kornhuber, K., Beobide-Arsuaga, G., Luo, F., and Coumou, D. (2018). Accelerated western european heatwave trends linked to more-persistent double jets over eurasia. *Nature Communication*, page 3851.

Schlenker, W. and Lobell, D. B. (2010). Robust negative impacts of climate change on african agriculture. *Environmental Research Letters*, 5(1):014010.

Schlenker, W. and Roberts, M. J. (2009). Nonlinear temperature effects indicate severe damages to us crop yields under climate change. *Proceedings of the National Academy of sciences*, 106(37):15594–15598.

Singhal, P. (2024). Inform me when it matters: Cost salience, energy consumption, and efficiency investments. *Energy Economics*, 133:107484.

Welch, J. R., Vincent, J. R., Auffhammer, M., Moya, P. F., Dobermann, A., and Dawe, D. (2010). Rice yields in tropical/subtropical asia exhibit large but opposing sensitivities to minimum and maximum temperatures. *Proceedings of the National Academy of Sciences*, 107(33):14562–14567.

Wu, J. C. and Xia, F. D. (2017). Time-varying lower bound of interest rates in europe. *Chicago Booth Research Paper*, (17-06).

Wu, J. C. and Xia, F. D. (2020). Negative interest rate policy and the yield curve. *Journal of Applied Econometrics*, 35(6):653–672.

Zohner, C. M., Mo, L., Renner, S. S., Svenning, J.-C., Vitasse, Y., Benito, B. M., Ordonez, A., Baumgarten, F., Bastin, J.-F., Sebald, V., Reich, P. B., Liang, J., Nabuurs, G.-J., de Miguel, S., Alberti, G., Antón-Fernández, C., Balazy, R., Brändli, U.-B., Chen, H. Y. H., Chisholm, C., Cienciala, E., Dayanandan, S., Fayle, T. M., Frizzera, L., Gianelle, D., Jagodzinski, A. M., Jaroszewicz, B., Jucker, T., Kepfer-Rojas, S., Khan, M. L., Kim, H. S., Korjus, H., Johannsen, V. K., Laarmann, D., Lang, M., Zawila-Niedzwiecki, T., Niklaus, P. A., Paquette, A., Pretzsch, H., Saikia, P., Schall, P., Šebeň, V., Svoboda, M., Tikhonova, E., Viana, H., Zhang, C., Zhao, X., and Crowther, T. W. (2020). Late-spring frost risk between 1959 and 2017 decreased in north america but increased in europe and asia. *Proceedings of the National Academy of Sciences*, 117:12192–12200.

Online-Appendix

Appendix 1: A three-sector behavioral New Keynesian model with food subsistence consumption and energy

The empirical results on the differential impact of food and energy price shocks on prices motivate a model to understand the underlying mechanisms. In particular, a key finding of the main analysis is that weather shocks have a smaller impact on food prices compared to energy prices. One explanation is that if a weather shock directly raises energy prices, these higher energy costs cascade through other production sectors, causing overall price increases.

To this end, we introduce a three-sector New Keynesian model to analyze the temperature surprise-induced energy and food price shock mechanisms. We further incorporate so-called behavioral inattention in the spirit of Gabaix (2020), differentiating our model from standard New Keynesian DSGE frameworks, which typically assume that agents form perfectly rational expectations. Such an assumption is particularly restrictive, as it relies on agents possessing complete knowledge of all potential future states and their capability to devise fully state-contingent plans through solving intricate optimization problems. Moreover, most empirical analyses of survey data have consistently rejected the hypothesis of full information rational expectations (FIRE), as documented by Coibion and Gorodnichenko (2015), Bordalo et al. (2020), and Kohlhas and Walther (2021). Behavioral inattention implies a behavioral bias where errors arising from price uncertainty indicate that consumers hold imperfect expectations regarding future prices. We believe that this is important for energy and food price shocks. Based on a large quasi-experimental setting for Germany, Singhal (2024) identifies salience cycles in heating bills lasting up to four months, likely reflecting short-lived consumer attention toward heating energy costs, which dissipates during periods when heating is not in use.

We also include food subsistence consumption as suggested by Portillo et al. (2016). Finally, our model also acknowledges the fact that the nominal interest rate is constrained

at the zero lower bound (ZLB). Energy is produced with green and dirty inputs and is bundled to an energy input that is used in the production sector for food, services, and energy for consumption services. As discussed in this paper, the food sector and energy prices are particularly vulnerable to temperature shocks. Therefore, this section examines the impact of a weather shock on food productivity and clean energy prices.

As demonstrated, our simple model replicates the key empirical patterns identified in this study. Food prices show the strongest reaction to a temperature shock, exerting a marked short-run influence on headline inflation, while other components remain largely unaffected. The model further predicts that this inflationary impact is temporary: headline inflation rises sharply at first, then follows a hump-shaped path before returning to baseline. As discussed in Section 5.2.1, this pattern reflects demand effects that materialize about five months after the initial food price increase. Likewise, a temperature shock that raises clean or brown resource prices feeds directly into higher energy (direct effect) and food prices (indirect effect), causing a short-lived spike in headline inflation. The effect on clean energy prices is more pronounced than on brown energy, reflecting the model's calibration to Germany's relatively green energy mix. In line with our empirical results in Section 5.2.2, these effects dissipate over time.

7.1 Cognitive Discounting

We assume that agents exhibit cognitive discounting when thinking about economic developments far into the future because agents cannot fully understand events that will take place in the very distant future, and, thus, progressively shrink those events toward steady-state values. In other words, agents are fully rational for steady state variables but act bounded rationally (partially myopic) to deviations from the deterministic steady state. In formal terms, deviations from the steady-state value of a variable that are expected to happen k periods in the future are discounted by an exogenously given factor m^k, where $m \in (0, 1)$ is a measure of the strength of cognitive discounting. Let X_t denote the state vector of the

economy. The log-linearized and demeaned law of motion can be written as

$$X_{t+1} = \Gamma X_t + \epsilon_{t+1}, \tag{11}$$

where Γ is a deterministic matrix of coefficients and ϵ_{t+1} shows a vector of mean-zero innovations. Instead, a behavioral agents perceives instead

$$X_{t+1} = m(\Gamma X_t + \epsilon_{t+1}). \tag{12}$$

According to Lemma 1 in Gabaix (2020), behavioral agents form expectations

$$\mathbb{E}_t^b[X_{t+k}] = m^k \mathbb{E}_t[X_{t+k}] = m^k \Gamma^k X_t, \tag{13}$$

where $\mathbb{E}_t^b$ and $\mathbb{E}_t$ denotes the behavioral and rational expectation's operator, respectively.

7.2 Households

Consider a representative, cognitively constrained household that derives utility from stochastic processes of aggregate consumption $\{\hat{C}_t\}$, labor $\{L_t\}$, and holdings of a nominal Bond $\{B_{t+1}\}$ according to the following expected utility function

$$\mathbb{E}_t^b \sum_{t=0}^{\infty} \beta^t \left[\ln(\tilde{C}_t) - \chi \frac{L_t^{1+\nu}}{1+\nu} \right], \tag{14}$$

where $\beta \in (0,1)$ denote the subjective discount factor, $\nu > 0$ and $\chi \in (0,1]$. The household chooses stochastic processes of bond holdings and consumption to maximize utility subject to the following budget constraint

$$P_{F,t}C_{F,t} + P_{N,t}C_{N,t} + P_{E,t}C_{E,t} + B_{t+1} = W_t L_t + \Pi_{F,t} + \Pi_{N,t} + \Pi_{E,t} + R_{t+1}B_t + Tr_t, \tag{15}$$

and the composition of $\tilde{C}_t$:

$$\tilde{C}_t = \Omega(C_{F,t} - \bar{C}_F)^{\alpha_F} C_{N,t}^{\alpha_N} C_{E,t}^{1-\alpha_N-\alpha_F}, \tag{16}$$

with $\Omega := \alpha_F^{-\alpha_F}\alpha_F^{-\alpha_F}(1-\alpha_N-\alpha_F)^{-(1-\alpha_N-\alpha_F)}$ as a scaling parameter. Note that $\bar{C}_F$ denotes the subsistence level of food. B_0 is exogenously given, $P_{F,t}$ presents the price of the final good produced in the temperature exposed sector, while $P_{N,t}$ shows the price of the final good produced in the non-temperature exposed sector. $P_{E,t}$ represents the price for energy consumption.

First-order conditions are given by

$$C_t: \quad \Lambda_t^{-1} = \tilde{C}_t \tilde{P}_t, \tag{17}$$

$$L_t: \quad \chi L_t^{\nu} = \Lambda_t \tilde{W}_t, \tag{18}$$

$$B_{t+1}: \quad \Lambda_t = \beta E_t[\Lambda_{t+1} R_t], \tag{19}$$

together with the TVC (no Ponzi scheme) that must hold in order to ensure that this programme has a solution. Λ_t denotes the marginal utility of consumption.

We can use the first-order conditions to derive the following relationships that govern the consumer's decisions but are not actually observed:

$$1 = \beta R_t E_t \left[\left(\frac{\tilde{C}_{t+1}}{\tilde{C}_t} \right)^{-1} \frac{\tilde{P}_t}{\tilde{P}_{t+1}} \right], \tag{20}$$

$$C_{F,t} = \bar{C}_F + \alpha_F \left(\frac{P_{F,t}}{\tilde{P}_t} \right)^{-1} \tilde{C}_t, \tag{21}$$

$$C_{N,t} = \alpha_N \left(\frac{P_{N,t}}{\tilde{P}_t} \right)^{-1} \tilde{C}_t, \tag{22}$$

$$C_{E,t} = (1-\alpha_N-\alpha_F) \left(\frac{P_{E,t}}{\tilde{P}_t} \right)^{-1} \tilde{C}_t, \tag{23}$$

with $\tilde{P}_t = P_{F,t}^{\alpha_F} P_{N,t}^{\alpha_N} P_{E,t}^{1-\alpha_N-\alpha_F}$ as the perceived consumption price index (see Portillo et al.

(2016)) that arises from utility maximization of the representative household and which is not equal to the *measured* price index P_t that is defined as follows:

$$P_t = \left(\frac{C_{F,t}}{C_t}\right) P_{F,t} + \left(\frac{C_{N,t}}{C_t}\right) P_{N,t} + \left(\frac{C_{E,t}}{C_t}\right) P_{E,t}, \tag{24}$$

with *measured* consumption C_t given as

$$C_t = \frac{P_F}{P} C_{F,t} + \frac{P_N}{P} C_{N,t} + \frac{P_E}{P} C_{E,t}, \tag{25}$$

where P_F, P_N and P_E respectively denote the steady-state prices for food, service and energy consumption, while and P is the economy-wide measured price indices. As noted by Portillo et al. (2016), for the consumer's decisions, ˜variables are relevant but - in contrast to variables without a ˜- are not actually observed.

7.3 Energy

For the sake of simplicity, we assume that energy producers and providers work in a perfectly competitive environment. The energy sector consists of two energy provider: The first - the clean energy provider - uses a renewable resource $X_{CP,t}$ such as wind or solar to produce output $E_{CP,t}$ and purchased at price $P_{CP,t}$, the second - the dirty energy provider - uses an non-renewable source $X_{Wo,t}$ such as oil or gas that is purchased at $P_{XWo,t}$ and produces $E_{Wo,t}$. The energy producer bundles $E_{CP,t}$ and $E_{Wo,t}$ and produces E_t that is, in turn sold on the spot market at price $P_{E,t}$. The prices of both resources are exogenous, and supply is perfectly elastic at that price. The energy input prices $P_{XWo,t}$ and $P_{XCP,t}$ are both subject to exogenous shocks. Finally, we assume that households own both resources.

7.3.1 Energy producer

The energy producer uses a CES production technology to produce the quantity of energy E_t:

$$E_t = \left[\kappa^{\frac{1}{\rho}} E_{CP,t}^{\frac{\rho-1}{\rho}} + (1-\kappa)^{\frac{1}{\rho}} E_{Wo,t}^{\frac{\rho-1}{\rho}}\right]^{\frac{\rho}{\rho-1}}, \tag{26}$$

where ρ is the elasticity of substitution between the two types of energy sources and κ is the relative weight in the bundle. The demand functions of the respective types of energy sources are given as

$$E_{CP,t} = \kappa \left(\frac{P_{CP,t}}{P_{E,t}}\right)^{-\rho} E_t \tag{27}$$

$$E_{W,t} = (1-\kappa) \left(\frac{P_{Wo,t}}{P_{E,t}}\right)^{-\rho} E_t \tag{28}$$

7.3.2 Energy input provider

For sake of simplicity, both energy provider $ep = \{CP, Wo\}$ use a linear technology to produce energy inputs for the energy producer

$$E_{ep,t} = Z_{ep,t} X_{ep,t}, \tag{29}$$

where $Z_{ep,t}$ is a provider specific productivity factor. The household owns resources X_t, where we assume that a constant fraction (ϖ) $1-\varpi$ of energy inputs X_t comprises a (non)-renewable resource, i.e. $X_{Wo,t} = \varpi X_t$ and $X_{Cp,t} = (1-\varpi)X_t$.

The profits of the energy producer Wo can be expressed as $P_{Wo,t}E_{Wo,t} - P_{XWo,t}X_{Wo,t}$, while the profits for the energy producer CP are expressed as $P_{CP,t}E_{CP,t} - P_{XCP,t}X_{CP,t}$. Solving the cost minimization problem yields the marginal costs of both providers as $MC_{ep} = \frac{P_{Xep,t}}{Z_{ep,t}}$. Finally, substituting the demand functions (27) and (28) in $P_{e,t}E_t = \sum_{ep} P_{ep,t}E_{ep,t}$

yields the energy price index

$$P_{e,t} = \left[\kappa P_{CP,t}^{1-\rho} + (1-\kappa) P_{Wo,t}^{1-\rho}\right]^{\frac{1}{1-\rho}}. \tag{30}$$

Finally, we impose that log-linearized technology $\hat{Z}_{ep,t}$ follows a first-order auto-regressive process

$$\hat{Z}_{ep,t} = \rho_{Z,ep} \hat{Z}_{ep,t-1} + \epsilon_{ep,t}, \tag{31}$$

with $\rho_{Z,ep} \in (0,1)$. $\epsilon_{ep,t}$ is a iid normally distributed with mean zero and variance $\sigma^2_{Z,ep}$ food sector shock.

7.4 The food sector

The food sector operates under perfect competition and flexible prices. The sector uses energy $E_{F,t}$ and labor $N_{F,t}$ to produce the output $Y_{F,t}$ with the following Cobb-Douglas technology that features labour-augmenting technological progress:

$$Y_{F,t} = A_{F,t} (AL_{F,t})^{\gamma} E_{F,t}^{1-\gamma}, \tag{32}$$

with $\gamma \in (0,1)$ as the labor share, A as the economy-wide labour-augmenting productivity A[24]. We assume that log-linearized technology in the food sector, $\hat{A}_{F,t}$ follows a first-order auto-regressive process

$$\hat{A}_{F,t} = \rho_{AF} \hat{A}_{F,t-1} + \epsilon_{AF,t}, \tag{33}$$

with $\rho_{AF} \in (0,1)$. $\epsilon_{AF,t}$ is a iid normally distributed with mean zero and variance σ^2_{AF} food sector shock.

[24] We assume that A is constant in our short-run analysis around the long-run steady-state that corresponds to different values for A.

7.5 The service sector

7.5.1 Final good firms

The service affected sector produces an output $Y_{N,t}$ using inputs of the intermediate goods according to

$$Y_{N,t} = \left[\int_0^1 (Y_{N,t}^j)^{\frac{\iota-1}{\iota}} dj \right], \tag{34}$$

where $\iota > 1$ denotes the elasticity of substitution among differentiated goods and Y_t^j is the input of the intermediate good $j \in [0, 1]$. Final-good firms are competitive and maximize profits. Cost minimization yields the following demand for intermediate good j:

$$Y_{N,t}^j = \left(\frac{P_{N,t}^j}{P_{N,t}} \right)^{-\iota} Y_{N,t}. \tag{35}$$

Moreover, the zero profit condition implies that

$$P_{N,t} = \left[\int_0^1 (P_{N,t}^j)^{-(\iota-1)} dj \right]^{\frac{1}{1-\iota}}. \tag{36}$$

7.5.2 The behavioral intermediate good firms

Behavioral intermediate goods firms produce and sell differentiated products to final good firms in a monopolistically competitive goods market. A firm uses a constant-returns-to-scale production function to produce the non-temperature affected good j:

$$Y_{N,t}^j = (AL_{N,t}^j)^{\gamma} (E_{N,t}^j)^{1-\gamma}, \tag{37}$$

with $\gamma \in (0, 1)$. $E_{N,t}^j$ is energy used by firm j in the N sector. The firm faces a downward-sloping demand function (35). Intermediate goods firms solve a static two-stage problem. Firstly, the costs minimization and, secondly, the profit maximization. The nominal cost function $Cost_t^j$ of firm j is given by $Cost_t^j = P_{E,t} E_{N,t}^j + W_{N,t} L_{N,t}^j$. Combining the first-order

conditions of the cost minimization problem yields

$$\frac{P_{E,t}E^j_{N,t}}{1-\gamma} = \frac{W_{N,t}L^j_{N,t}}{\gamma}. \tag{38}$$

Moreover, solving the first-order conditions for $L^j_{N,t}$ and $E^j_{N,t}$ allows to rewrite the production function as

$$Y^j_{N,t} = \left(\frac{MC^j_{N,t}(1-\gamma)Y^j_{N,t}}{P_{E,t}}\right)^{1-\gamma}\left(\frac{AMC^j_{N,t}(\gamma)Y^j_{N,t}}{W_{N,t}}\right)^{\gamma},$$

where $MC^j_{N,t}$ is the cost minimization's Lagrange multiplier that represents the firm's j nominal marginal costs, since it measures the increase in the cost function as output $Y^j_{N,t}$ marginally increases. Solving the latter expression for $MC^j_{N,t}$ yields

$$MC^j_{N,t} = (A\gamma)^{-\gamma}(1-\gamma)^{-(1-\gamma)}P^{1-\gamma}_{E,t}W^{\gamma}_{N,t}. \tag{39}$$

From (39) we observe that all intermediate firms face the same prices and employ the same production technology. Hence, $MC^j_{N,t} = MC_{N,t}\ \forall\ j$. In real terms, marginal cost are given as $mc_{N,t} \equiv \frac{MC_{N,t}}{P_{N,t}}$ and firm's j nominal cost function can be re-expressed as $Cost^j_t(Y^j_{N,t}) = MC^j_{N,t}Y^j_{N,t}$.

Next, we turn to the pricing decisions of the firms. Under flexible prices, each intermediate firm j chooses $P^j_{N,t}$, $Y^j_{N,t}$, $L^j_{N,t}$ and $E^j_{N,t}$ in order to maximize profits subject to the final goods producer's demand schedule. The familiar first-order condition of the associated problem reads $P^j_{N,t} = \left(\frac{\iota}{\iota-1}\right)MC_{N,t}$, for all firms $j \in [0,1]$, where $\left(\frac{\iota}{\iota-1}\right)$ is a constant mark-up over marginal costs. Hence, the optimal price chosen by each firm j is given by $P^{*j}_{N,t} = \left(\frac{\iota}{\iota-1}\right)MC_{N,t}$, because marginal costs $MC_{N,t}$ do not depend on firm j.

Following Calvo (1983), in each period, a firm adjusts its price with a constant probability $1-\theta$ and does not adjust its price with a constant probability θ. Using the law of large numbers, we can interpret θ as the faction of firms that do not adjust their prices. Let $P^*_{N,t}$ the price that is chosen by firm j in period t. If a behavioral firm j obtains a random signal

in t, it chooses $P^*_{N,t}$ to maximize the discounted present value of real profits:

$$\max_{P^*_{N,t}} \mathbb{E}^b_t \left\{ \sum_{k=0}^{\infty} (\beta\theta)^k \Lambda_{t+k} \left[\left(\frac{P^{*j}_{N,t}}{P_{N,t}} \right) Y_{N,t+k} [P^{*j}_{N,t} - mc^j_{N,t+k}(1-\tau)] \right]^{-\iota} \right\}, \tag{40}$$

where Λ_{t+k} is the stochastic discount factor, τ is an employment subsidy, and $mc_{N,t+k}$ denotes the real marginal costs in period $t+k$ of firm j that last set its price at $P^{*j}_{N,t}$ in period t.

Under Calvo price setting and by the law of large numbers, we can rewrite (36) and obtain an aggregate price relationship

$$P^{1-\iota}_{N,t} = \theta P^{1-\iota}_{N,t-1} + (1-\theta)(P^{*j}_{N,t})^{1-\iota}. \tag{41}$$

Thus, a fraction $1-\theta$ of firms adjust prices to the new level $P^{*j}_{N,t}$, while a fraction θ keeps prices at the previous period's level.

7.6 Monetary Policy

Monetary policy authority is constrained by the zero lower bound (ZLB). The (truncated) Taylor rule is given by

$$R_t = \max[R^{Taylor}_t; 0] \tag{42}$$

Thus, monetary authority sets interest to zero when the economy is in the ZLB. However, out of the ZLB, the interest rate is determined by

$$R^{Taylor}_t = \left[\left(\frac{\pi_t}{\pi} \right)^{\phi_\pi} \left(\frac{Y_t}{Y} \right)^{\phi_Y} \right]^{1-\rho_R} \left(\frac{R_{t-1}}{R} \right)^{\rho_R} R, \tag{43}$$

where $0 < \phi_y < 1$ and $\phi_\pi > 1$ are monetary policy coefficients and $0 < \rho_R < 1$ governs the degree of nominal interest rate smoothing. Y, R and π each denote non-stochastic, steady-state variables.

7.7 Equilibrium

Our model consists of the labor and final goods market. Without investments into physical capital, the market clearing conditions are simply

$$C_{F,t} = Y_{F,t},\ C_{N,t} = Y_{N,t}, C_{E,t} = E_{C,t} \text{ and } E_t = E_{C,t} + E_{N,t} + E_{F,t} \text{ and } L_t = L_{F,t} + \int_0^1 L_{N,t}^j dj. \tag{44}$$

For simplicity, we further assume that real resource rents are fully redistributed to households, the resource owners, as additional source of income. This implies that real gdp reads as

$$\begin{aligned} Y_t &= p_f Y_{F,t} + p_n Y_{N,t} p_n + p_e E_{C,t}, \\ &= p_f C_{F,t} + p_n C_{N,t} + p_e C_{E,t}, \end{aligned} \tag{45}$$

with $p_f = \frac{P_f}{P^Y}$, $p_n = \frac{P_n}{P^Y}$ and $p_e = \frac{P_E}{P^Y}$. Note that we assume that the GDP deflator equals the CPI deflator ($P_t = P_t^Y$) in order to avoid the paradoxical situation that if energy price experiences an upward shock, the GDP deflator decreases. For simplicity, we assume that a constant fraction of energy demand is devoted to the production of food, services and for consumption, i.e. $E_{F,t} = \varphi_F E_t$, $E_{N,t} = \varphi_N E_t$ and $E_{C,t} = \varphi_C E_t$. Finally, bond markets clear.

7.8 Steady state

In this section we derive a non-inflationary steady steate, which implies that $p_{E,t} = p_{N,t} = p_{F,t} = p_{CP,t} = p_{Wo,t} = p_{XWo,t} = p_{XCP,t} = p = 1 \forall t$ with the gross inflation rate $\pi_t = \frac{P_t}{P_{t-1}} = 1$. Moreover, we set $A_{F,t} = 1$. Inter alia, these assumptions ensure that measured real wages are equal to the real wages that result from optimization, i.e. $W_t = W_{N,t} = W_{F,t} = W = \tilde{W}_t = w$. Further, $\pi = 1$ also implies that $\tilde{\pi} = 1$. Next, we set $\tau = \frac{1}{\iota}$ in order to remove the market power by monopolistic competition in the service sector (see expression (40)).

As in the neoclassical growth model, we observe a linear relationship between real wages and

aggregate labor productivity A:

$$w = W = \left[\gamma^{\gamma}(1-\gamma)^{1-\gamma}\right]^{\frac{1}{\gamma}} A = \Theta A, \tag{46}$$

with $\Theta := \left[\gamma^{\gamma}(1-\gamma)^{1-\gamma}\right]^{\frac{1}{\gamma}}$.

Next, we use (18) to derive a relationship between aggregate labor productivity A and measure consumption c. From (18) we have $\chi N^{\nu} = W\tilde{C}$. Together with $C = \bar{C}_F + \tilde{C}$[25] and (46), we obtain a non-linear relationship between aggregate consumption and the economy-wide productivity A (with an elasticity below one):

$$\chi\gamma^{\psi}C^{\psi}(C - \bar{C}_F) = \Theta^{1+\psi}A^{1+\psi}. \tag{47}$$

Labor supply is given by

$$L = \left[\frac{\Theta A}{\chi(C - \bar{C}_F)}\right]^{\frac{1}{\nu}}, \tag{48}$$

indicating that when $C \to \bar{C}_F$, the income effect dominates the substitution effect in the labor supply decision as agents work more to finance their subsistence needs. Next, solving (38) for $E^j_{N,t}$, using this in (37), and solving this for $L^j_{N,t}$, and since all firms j solve the same optimization problem, in the steady state, we find that $L_N = \frac{Y_N}{A\left(\frac{1-\gamma}{\gamma}\right)\frac{P_E}{W}}$. Similarly, solving the cost mimization problem of the food sector, we find $L_F = \frac{Y_F}{A\left(\frac{1-\gamma}{\gamma}\right)\frac{P_F}{W}}$. Next, the share of labor employed in the food or service sector is given by $\frac{L_N}{L}$. Together with the equilibrium conditions (44), we find that in the steady state

$$\epsilon_F := \frac{L_F}{L} = \frac{C_F}{C} = \alpha_F + (1-\alpha_F)\frac{\bar{C}_F}{C}, \text{ with } \epsilon_F \geq \alpha_F, \tag{49}$$

$$\epsilon_N := \frac{L_N}{L} = \frac{C_N}{C} = \alpha_N\left(1 - \frac{\bar{C}_F}{C}\right), \tag{50}$$

$$\epsilon_E := \frac{C_E}{C} = \alpha_E\left(1 - \frac{\bar{C}_F}{C}\right), \tag{51}$$

[25] This follows from the combination of (25) with (23) and (21).

where for the last expression on the right hand side, we use the fact that after the price normalization, we observe a simple linear relationship between measured aggregate consumption C and $\tilde{C}$ as $C = C_F + \tilde{C}$. It is obvious that $\epsilon_N + \epsilon_E + \epsilon_F = 1$. If steady state consumption increases, ϵ converges from above to α_F. If subsistence consumption is absent ($\bar{C}_F = 0$), we have that $\epsilon_k = \alpha_k$ for $k = \{F, N, E\}$, and, similar as in the neoclassical growth model, we observe a linear relationship between aggregate consumption and the economy-wide productivity A (see (47)).

7.9 Log-linear approximation

In this section, we describe the log-linearization of the model.

7.9.1 Behavioral IS curve

In contrast to the standard behavioral New Keynesian setting suggested by Gabaix (2020), in this model, the behavioral IS-curve exhibits two modifications due to the existence of subsistence consumption in the food sector. First, note that

$$\hat{C}_t = \left[\frac{1-\epsilon_F}{1-\alpha_F}\right]\hat{\tilde{C}}_t. \tag{52}$$

Next, there is a difference between the inflation rate that matters for the private sector decisions ($\tilde{\pi}_t$) and measured inflation (π_t). Log-linearization of this relationship yields

$$\hat{\tilde{\pi}}_t = \hat{\pi}_t + \underbrace{\left(\frac{\epsilon_N\alpha_F - \alpha_N\epsilon_F}{\epsilon_N}\right)}_{:=\Psi_F}\Delta\hat{p}_{F,t} + \underbrace{\left(\frac{\epsilon_N\alpha_E - \alpha_N\epsilon_E}{\epsilon_N}\right)}_{:=\Psi_E}\Delta\hat{p}_{E,t}, \tag{53}$$

where we can show by using (49)-(51) that $\Psi_F < 0$ and $\Psi_E = 0$. Reflecting (49)-(51), expression (53) reduces to $\hat{\tilde{\pi}}_t = \hat{\pi}_t$ while expression (52) simplifies to $\hat{C}_t = \hat{\tilde{C}}_t$ if subsistence consumption does not play a role, i.e. $\bar{C}_F = 0$.

Log-linearization of (45), using (53) and inserting the log-linearized version of (20) yields

the behavioral, forward-looking IS curve:

$$\hat{Y}_t = -\left[\frac{1-\epsilon_F}{1-\alpha_F}\right]\mathbb{E}_t^b\left(\hat{R}_t - \hat{\pi}_{t+1} + \Psi_F\Delta\hat{p}_{F,t+1} + \Psi_E\Delta\hat{p}_{E,t+1}\right) + \mathbb{E}_t^b[\hat{Y}_{t+1}]. \quad (54)$$

Next, we apply Lemma 1 in Gabaix (2020): $\mathbb{E}_t^b[\hat{Y}_t] = m\mathbb{E}_t[\hat{Y}_t]$. Hence, (55) can be rewritten as

$$\hat{Y}_t = -\left[\frac{1-\epsilon_F}{1-\alpha_F}\right]\left(\hat{R}_t - m\mathbb{E}_t[\hat{\pi}_{t+1} + \Psi_F\Delta\hat{p}_{F,t+1} + \Psi_E\Delta\hat{p}_{E,t+1}]\right) + m\mathbb{E}_t[\hat{Y}_{t+1}]. \quad (55)$$

Note that due the the subsistence consumption $\bar{C}_F > 0$, the intertemporal elasticity of substitution for output $-\left[\frac{1-\epsilon_F}{1-\alpha_F}\right]$ is smaller than one provided that $\epsilon_F > \alpha_F$. Moreover, for $\epsilon_F > \alpha_F$, there is a wedge between measured inflation and experienced inflation (see 53).

Log-linearization of (18) yields the labor supply condition:

$$\begin{aligned}\nu\hat{L}_t &= \hat{W}_t - \hat{\tilde{P}}_t - \hat{\tilde{C}}_t \\ &= \hat{W}_t - \hat{P}_t - \Psi_F\hat{p}_{F,t} - \Psi_E\hat{p}_{E,t} - \hat{\tilde{C}}_t \\ &= \hat{w}_t - \Psi_F\hat{p}_{F,t} - \Psi_E\hat{p}_{E,t} - \left[\frac{1-\alpha_F}{1-\epsilon_F}\right]\hat{C}_t, \end{aligned} \quad (56)$$

where $w_t = \frac{W_t}{P_t}$. Next, using the log-linearized versions of (21) and (23), we can derive the sector-specific consumption demand equations as follows:

$$\hat{C}_{F,t} = \left[\frac{\alpha_F(1-\epsilon_F)}{\epsilon_F(1-\alpha_F)}\right][-(1-\Psi_F)\hat{p}_{F,t} + \Psi_E\hat{p}_{E,t}] + \left[\frac{\alpha_F}{\epsilon_F}\right]\hat{C}_t, \quad (57)$$

$$\hat{C}_{N,t} = \left[\left(\frac{\epsilon_F}{\epsilon_N} + \Psi_F\right)\hat{p}_{F,t} + \left(\frac{\epsilon_E}{\epsilon_N} + \Psi_E\right)\hat{p}_{E,t}\right] + \left[\frac{1-\alpha_F}{1-\epsilon_F}\right]\hat{C}_t, \quad (58)$$

and

$$\hat{C}_{E,t} = [-(1-\Psi_E)\hat{p}_{E,t} + \Psi_F\hat{p}_{F,t}] + \left[\frac{1-\alpha_F}{1-\epsilon_F}\right]\hat{C}_t, \quad (59)$$

Equations (57)-(59) together with (49)-(51) imply $\hat{C}_t = \hat{C}_{F,t}\epsilon_F + \hat{C}_{N,t}\epsilon_N + \hat{C}_{E,t}\epsilon_E$.

The remaining log-linearized equations are standard. The supply of food and services can be derived from the sector-specific profit maximization problems:

$$\left[\frac{1-\gamma}{\gamma}\right]\hat{Y}_{F,t} = \left[\frac{1-\gamma}{\gamma}\right]\hat{E}_{F,t} + \hat{p}_{F,t} + \frac{1}{\gamma}\hat{A}_{F,t} - \hat{w}_t, \tag{60}$$

$$\left[\frac{1-\gamma}{\gamma}\right]\hat{Y}_{N,t} = \left[\frac{1-\gamma}{\gamma}\right]\hat{E}_{N,t} \underbrace{- \left[\frac{\epsilon_F}{\epsilon_N}\right]\hat{p}_{F,t} - \left[\frac{\epsilon_E}{\epsilon_N}\right]\hat{p}_{E,t}}_{+\hat{p}_{N,t}} - \hat{w}_t - \hat{\mu}_t, \tag{61}$$

where μ_t denotes the markup in the non-food sector.

The demand for energy in the food and service sector reads as:

$$\begin{aligned}
\hat{E}_{F,t} &= -\hat{p}_{E,t} + \hat{p}_{F,t} + \hat{Y}_{F,t} && (62)\\
\hat{E}_{N,t} &= -\hat{p}_{E,t} + \hat{p}_{N,t} + \hat{Y}_{N,t} && (63)\\
&= -\hat{p}_{E,t} - \left[\frac{\epsilon_F}{\epsilon_N}\right]\hat{p}_{F,t} - \left[\frac{\epsilon_E}{\epsilon_N}\right]\hat{p}_{E,t} + \hat{Y}_{N,t}. && (64)
\end{aligned}$$

Based on marginal costs in the energy production sector, we can derive a log-linear relationship between the price of energy types and resource prices and energy-specific technology:

$$\hat{p}_{ep,t} = -\hat{Z}_{ep,t} + \hat{p}_{Xep,t}, \tag{65}$$

with $ep = \{CP, Wo\}$. Moreover, energy demand in the energy sector reads as

$$\begin{aligned}
\hat{E}_{CP,t} &= \rho(\hat{p}_{E,t} - \hat{p}_{CP,t}) + \hat{E}_t && (66)\\
\hat{E}_{Wo,t} &= \rho(\hat{p}_{E,t} - \hat{p}_{Wo,t}) + \hat{E}_t, && (67)
\end{aligned}$$

with

$$\hat{p}_{E,t} = \kappa\hat{p}_{CP,t} + (1-\kappa)\hat{p}_{Wo,t}. \tag{68}$$

Reflecting on equations (65)-(68), we observe that when resource prices increase, energy input prices subsequently rise. This price increase induces a partial substitution between the different inputs used in energy production, with the extent of substitution determined by the parameter ρ.

7.10 Behavioral Phillips curve

Inflation in the service sector is determined by a new-Keynesian, behavioral Philips curve:

$$\hat{\pi}_{N,t} = \beta \mathbb{E}_t^b[\hat{\pi}_{N,t+1}] + \frac{(1-\beta\theta)(1-\theta)}{\theta(1+b)}\hat{\mu}, \tag{69}$$

with $b := \frac{-\iota(1-\gamma)}{\gamma}$. Again, we apply Lemma 1 in Gabaix (2020) and rewrite (69) as

$$\hat{\pi}_{N,t} = \beta m \mathbb{E}_t[\hat{\pi}_{N,t+1}] + \frac{(1-\beta\theta)(1-\theta)}{\theta(1+b)}\hat{\mu}. \tag{70}$$

Note that differs from Gabaix (2020), because Benchimol and Bounader (2023) as well as Meggiorini (2023) have shown that the Phillips curve derived in Gabaix (2020) is not consistent with Lemma 1 in Gabaix (2020). Gabaix (2020) employs Lemma 1 for level variables, although Lemma 1 in Gabaix (2020) considers deviations from the steady state.

7.11 Additional relationships

Moreover, headline inflation is given by

$$\hat{\pi}_t = \hat{\pi}_{N,t} + \left(\frac{\epsilon_F}{\epsilon_N}\right)\Delta\hat{p}_{F,t} + \left(\frac{\epsilon_E}{\epsilon_N}\right)\Delta\hat{p}_{E,t}. \tag{71}$$

We also can make use of the definition of aggregate GDP to derive a relationship between aggregate employment L_t, energy production, and aggregate output Y_t:

$$\begin{aligned}\hat{Y}_t &= \gamma\hat{L}_t + \epsilon_F\hat{A}_{F,t} + (1-\gamma)[\epsilon_F\hat{E}_{F,t} + \epsilon_N\hat{E}_{N,t}] + \epsilon_E\hat{E}_{C,t} \\ &= \gamma\hat{L}_t + \epsilon_F\hat{A}_{F,t} + \hat{E}_t[1-\gamma(1-\epsilon_E)],\end{aligned} \tag{72}$$

where $\hat{L}_t = \epsilon_F \hat{L}_{F,t} + \epsilon_N \hat{L}_{N,t}$ and $\hat{Y}_t = \hat{C}_t = \epsilon_F \hat{Y}_{F,t} + \epsilon_N \hat{Y}_{N,t} + \epsilon_E \hat{E}_{C,t}$.

Finally, the log-linearized version of the interest rate rule given by (43) reads as:

$$\hat{R}_t = \max[\hat{R}_t^{Taylor}; -\bar{R}] \tag{73}$$

with

$$\hat{R}_t^{Taylor} = \rho_R \hat{R}_{t-1} + (1 - \rho_R)(\phi_\pi \hat{\pi}_t + \phi_y \hat{y}_t), \tag{74}$$

where $\bar{R} = \frac{1}{\beta}$ denotes the deterministic, steady-state gross interest rate.

7.12 Calibration

We calibrate the model on a monthly basis for the german economy. We follow Portillo et al. (2016) and calibrate the subsistence level of food consumption to $\bar{C}_F = 0.0099$. This value corresponds to OECD countries such as Germany. Moreover, we also follow Portillo et al. (2016) and pin down α_F to 0.0701. We set the share of the services sector in the total consumption bundle to $\alpha_N = 0.7$, to match the share of services in total production for the german economy, which was approximately 70% in 2024. This value equals to what Chafwehé et al. (2025) postulates for the U.S. economy. The next three calibrated are standard in the literature: The subjective discount factor is calibrated to $\beta = \left(\frac{1}{1.04}\right)^{\frac{1}{12}} = 0.9967$ (see Gali (2015), p. 67). The Calvo parameter, θ, is set to $\theta = 1 - \frac{1}{\left(\frac{1}{(1-3/4)3)}\right)} = 0.9167$ (see Gali (2015) , p. 67), while the inverse of the Frisch elasticity of labor supply, ν is set to 5 (Frisch elasticity of 0.2). As labor is supplied inelastically, χ is normalized to one. We follow the literature and set the labor income share γ for the food and service sector is set to 0.7 while the elasticity of substitution between different varieties, ι is set to 6.

The elasticity of substitution (eos) between clean and dirty energy inputs is set to 1.8 (see Papageorgiou et al. (2017)). Thus, clean and dirty energy goods are imperfect substitutes. The share of energy that is used for food and service production is set to 0.4. In Germany,

the fraction of clean energy in the energy bundle rises from 46.3 % in 2022 to 52,5% in 2023. We calibrate a value of 51% that is close to what we found for the year 2023 in Germany. According to the German statistical office[26], in 2021, the household sector has used 28% of energy production, while the service sector has used 32%. The manufacturing sector to which the food sector belongs used 39% of energy sector production.

The calibrated parameters for the interest rate rule $\phi_y = 0.5$, $\phi_\pi = 1.5$ and $\rho = 0.875$ are in line with existing literature and consistent with the Taylor Principle (see Gali (2015)).

We follow Gabaix (2020) and calibrate $m = 0.85$. This implies that an agent pays just over half the level of attention to an innovation arriving one year in the future relative to the attention paid to it today.

Chafwehé et al. (2025) report an autocorrelation coefficient for fossil fuel price shock of 0.494 for the U.S., while Pataracchia et al. (2023) and Bodenstein et al. (2011) for European countries report an autocorrelation coefficients of fossil price shocks between 0.85 and 0.95. The discrepancy can be partly explained by the different country focus and sample period discrepancies. Similarly, the autocorrelation of the TFP shock is significantly lower estimated by Chafwehé et al. (2025) with 0.407 compared to Pataracchia et al. (2023) and Bodenstein et al. (2011). We follow Pataracchia et al. (2023) and Bodenstein et al. (2011) and Gali (2015) and calibrate the autocorrelation coefficients for the exogenous shock process with respect to fossil and non-fossil input price shocks as $\rho_{XWo} = \rho_{XCP} = 0.95^{\frac{1}{3}}$, the autocorrelation coefficient for the monetary policy shock as $\rho_v = 0.5^{\frac{1}{3}}$ and the autocorrelation coefficients for the food and energy sector productivity shock as $\rho_{AF} = \rho_{Z,ep} = 0.9^{\frac{1}{3}}$. The corresponding standard deviations are all summarized in the lower part of Table 8.

[26] See https://www.destatis.de/EN/Themes/Economic-Sectors-Enterprises/Industry-Manufacturing/_node.html, accessed on 11th April 2025.

Table 8: Calibration

Parameter	Definition	Value
Household		
β	Subjective discount factor	0.9967
$\bar{C}_F$	Subsistence level of food consumption	0.0099
α_F	Non-subsistence food consumption share	0.0701
α_N	Non-subsistence service consumption share	0.7
ν	Inverse of Frisch elasticity of labor supply	5
Food sector		
γ	Labor income share	0.7
Service sector		
γ	Labor income share	0.7
ι	Elasticity of substitution between different varieties	6
Energy sector		
ρ	Eos between clean and dirty energy inputs	1.8
κ	Share of clean energy in energy bundle	0.51
φ_F	Share of energy used in the food sector	0.39
φ_N	Share of energy used in the service sector	0.32
φ_C	Share of energy for household consumption	0.28
Monetary policy		
ϕ_y	Taylor rule, output coefficient	0.5
ϕ_π	Taylor rule, inflation coefficient	1.5
ρ	Interest smoothing coefficient	0.875
Prices		
θ	Calvo parameter	0.9167
Behavioral		
m	Cognitive discount factor	0.85
Shocks		
ρ_{AF}	AR coefficient for food productivity shock	0.9655
ρ_{XWo}	AR coefficient fossil resource price shock	0.9830
ρ_{XCP}	AR coefficient non-fossil resource price shock	0.9830
$\rho_{Z,ep}$	AR coefficient for energy input productivity shock of type *ep*	0.9655
ρ_v	AR coefficient for monetary policy shock	0.7937
σ^2_{AF}	Std. dev. food productivity shock	0.0057
σ^2_{XWo}	Std. dev. fossil resource price shock	0.006
σ^2_{XCP}	Std. dev. non-fossil resource price shock	0.006
$\sigma^2_{Z,ep}$	Std. dev. energy input productivity shock of type *ep*	0.0057
σ^2_v	Std. dev. monetary policy shock	0.0833

7.13 Impulse response function analysis

Figure 12 illustrates the effects of a one percent decline in food sector productivity caused by a weather shock. Due to the presence of subsistence of food consumption (and the reduced substitutability with energy and service goods), relative price rises more sharply than it would in the absence of subsistence constraints. As a result, food production contracts less than in an environment without subsistence constraints. However, this comes at the expense of reduced output in the service and energy sectors. However, aggregate production contracts less compared to the food sector. The decline in food sector productivity also lowers the overall energy demand, as food, energy, and service sectors require less input. Consequently, both clean and dirty energy demand decreases while energy prices remain unaffected. Moreover, higher food prices initially drive an increase in headline inflation. However, after two periods, food price change is negative due to declining wages, which result from weakened labor demand. Meanwhile, core inflation rises as service sector firms gradually pass higher marginal costs onto final goods producers, leading to higher consumer prices in the service sector. The rise in headline inflation leads to an increase in the nominal interest rate. In summary, a weather shock that reduces food productivity leads to a short- and medium-term increase in both headline and core inflation, a decline in labor and energy demand, and unchanged energy prices.

Figure 13 summarizes the impact of a weather shock that raises exogenous clean resource prices(e.g. light wind that reduces supply). This might even has macroeconomic effects, because as previously mentioned, 52.5% of Germany's energy production in 2023 relies on renewables. Higher clean resource prices can result from adverse weather conditions that constrain supply.

On the real side of the economy, aggregate output declines as firms across all sectors reduce production. The overall rise in energy prices temporarily alters the energy mix in

Figure 12: Effects of a weather shock that negatively impacts food productivity. Variables are expressed in percentage deviations from their respective initial steady state. Nominal interest rate and inflation rates are in percentage point deviations from the initial steady state. Time on the horizontal axis is in months.

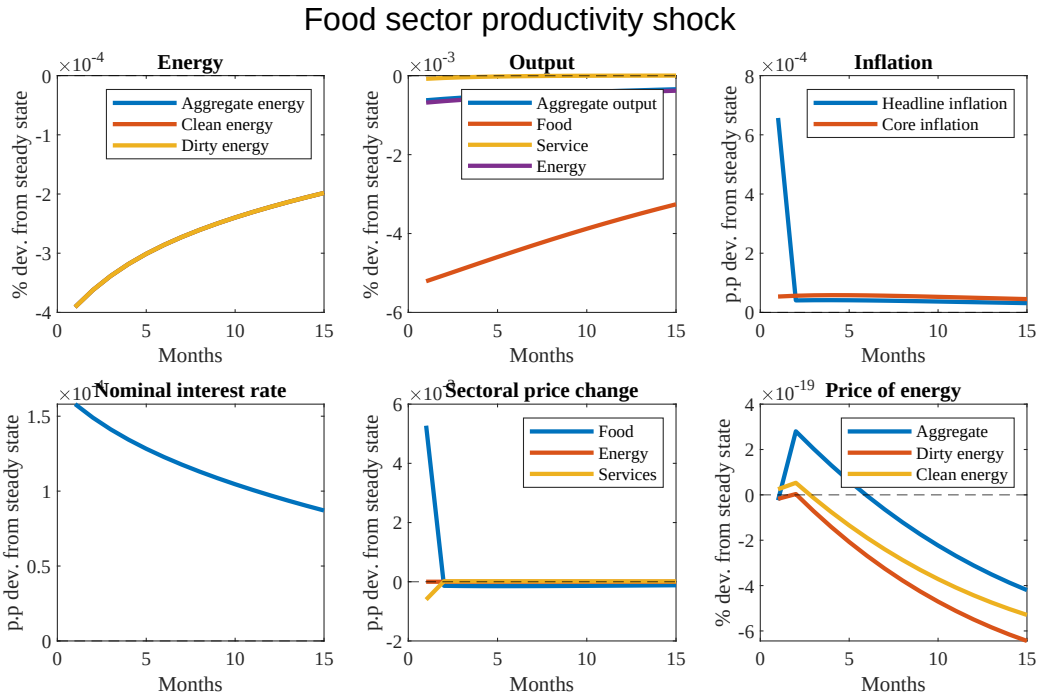

both consumption and production. Specifically, the increase in clean energy prices—driven by higher clean resource costs—encourages firms to shift from green to dirty energy. However, the price of dirty energy remains unchanged, as the wage decline (due to lower labor demand) offsets the price increase of dirty energy, which is driven by higher demand in the production sectors. Moreover, the shock to clean resource prices triggers an immediate rise in both core as well as headline inflation. Headline inflation increases as higher clean resource prices directly feed into higher energy and consumption prices. Consequently, headline inflation increases by 0.28 percentage points on impact before it slowly converges to its steady-state. Core inflation rises as intermediate-good producers gradually pass through the increase of marginal production costs to final good producers.

In summary, a weather shock that directly raises the prices of clean resources impacts clean energy, overall energy prices, and sector-specific prices (through the pass-through of

higher energy costs), while simultaneously causing a contraction in production. Increased costs of clean energy inputs encourage a shift toward dirtier energy sources. The resulting short-term rise in headline inflation is predominantly driven by higher energy and food prices, with these price effects proving persistent.

Figure 13: Effects of a weather shock that negatively impacts clean energy prices. Variables are expressed in percentage deviations from their respective initial steady state. Nominal interest rate and inflation rates are in percentage point deviations from the initial steady state. Time on the horizontal axis is in months.

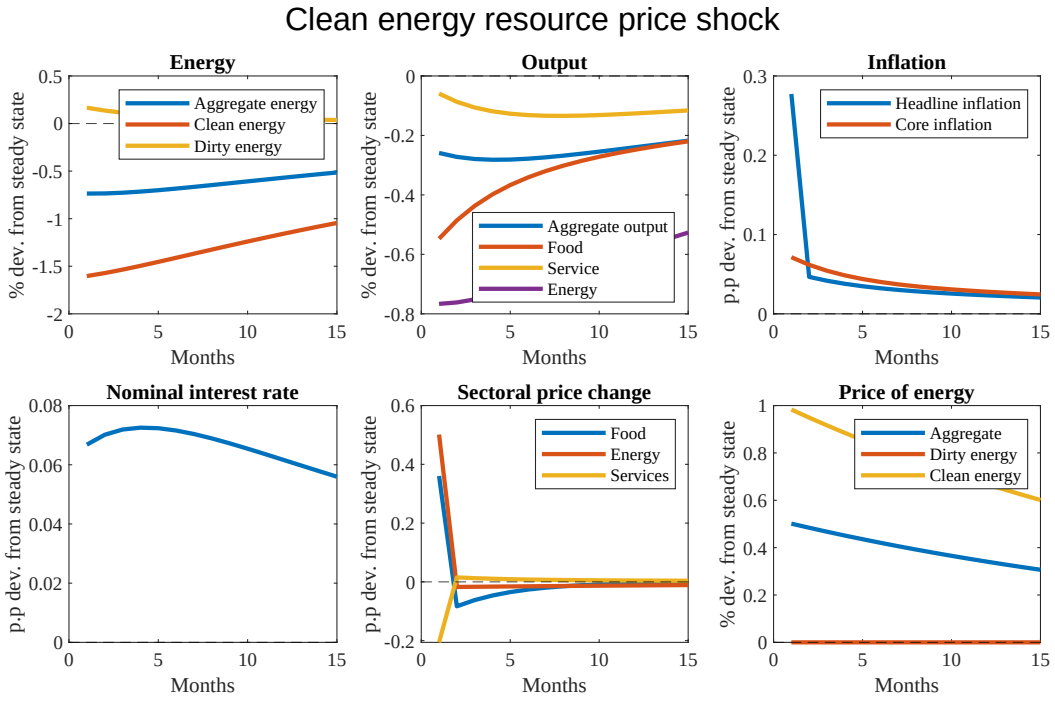

Appendix 2: Additional Robustness Exercises

A.2.1 Comparison with Temperature Anomalies

As a further robustness check, we compare our baseline results for our two shock types to another shock measure from the literature: temperature anomalies. Important to note is the fact that we adjusted the temperature anomalies to be comparable to our shocks. We do not compare the monthly temperature average to a historical period but rather to the temperature during the same month over the past five years. Thus, we still have agents who permanently adjust their expectations. Otherwise, it seems unsuitable to compare standard computed anomalies to our shock design. Regarding interpretation, it only makes sense to compare those anomalies to our hot extremes since both measure whether or how warm a month is, while our cold shock does the opposite. Here, our shock design shows its advantage of being able to measure explicitly both ends of the temperature distribution. We do focus on seasonal influences on headline, food, and energy inflation, as our most interesting baseline results were found using the specification from the equation (10). All in all, the impulse responses are pretty similar to our hot day shock. During winter and spring, food prices decrease, while a warm summer leads to an increase. Again, here we observe the typical S-shape behavior, where food price return to the pre-shock level and then even further decrease due to demand effects. For energy, the picture is also very much in line with our baseline results, where warmer months during fall, winter, and summer cause declining prices. Responses of core inflation are far less clear, where we cannot observe such strong patterns as for food and energy prices. Core inflation still appears to be driven by services, as both indices are moving in similar directions.

A.2.2 Different Weightings

In our main shock design, we aggregate our local weather shocks using population numbers as weights. The argument is simple: the more people live in a region, the more they are exposed

to certain weather conditions causing potential consequences (for example, higher energy demand). Nevertheless, one could think about other possibilities, moving away from the simple exposure of people argument. The most obvious might be focusing on the economic relevance of each region using GDP as weights. Economically stronger regions are therefore weighted more heavily, as any economic damage could be greater here and therefore have a greater impact on the macroeconomy. As a second alternative, we take the agricultural area, trying to capture the food channel shown in this paper. Regions more dependent on agriculture might suffer more from bad temperature values, dampening food production at a larger scale. While the agricultural area follows a similar idea as population, measuring the exposure to temperature conditions of a region, the GDP focuses purely on economic performance. Yearly regional data for all German "Landkreise" are taken from the inkar database. Since the data for agricultural land is only available for "Landkreise" from 2016 and is unlikely to change that much over time, we take the last observed value from 2021 for the entire sample.

Figure 15 presents the impulse responses for multiple price indices covered in this paper, where the local temperature shocks were aggregated using GDP as weights. In addition to that figure 16 shows the same plots, but aggregation was performed using agricultural area as weights. Comparing both figures with our baseline shock design and the respective impulse responses, we do not observe any changes qualitatively but only very small changes quantitatively. All identified channels are still present in both alternative aggregation procedures. Especially looking at food and energy prices, hot and cold extremes lead to opposite price responses depending on the calendar season. To highlight only a few patterns, during winter and spring, cold shocks increase food prices up to 0.5 percent, similar to before. For a hot summer, we still observe the S-shaped behavior, where food prices return to the pre-shock level after a sharp increase initially after the shock. Energy prices react most interestingly during winter, where we still observe the opposite response of warm and cold spells. As

expected, a cold winter increases energy prices, while a warm winter lowers energy demand and thus, energy prices decrease significantly up to one percent.

A.2.3 Different learning periods

As discussed in the main part of our paper, we ensure that the choice of our learning window does not drive the results. Thus, we construct the same types of shocks, except that the reference distribution used to determine whether a day is extreme includes not the past 5 years but instead 2 or 10 years, respectively. In this way we try to cover both extremes. People only rely on very recent events to form their expectations versus people looking further into the past to make a prediction. Apart from that, we perform the same local projection analysis as before.

Qualitatively, the results remain unchanged regardless of the chosen learning period. As can be seen in figure 17 for a 2-year learning period, warm winters decrease energy and food prices, the latter persistently for 9 months and up to 0.4 percent. During summer months, we still observe our S-shape behavior for food prices (increase of 0.3 percent on impact), which even significantly decreases 6 months after the shock. For the remaining indices and seasons, we do not see any significant variations. Turning to Figure 18, we observe similar patterns for the extended learning period of 10 years, with only minor quantitative differences.

A.2.4 Year on Year Inflation Rates

Figure 19 shows the results when using the year-on-year inflation rates of the respective CPI components as the dependent variable in our local projection framework. By performing this kind of additional robustness check, we account for the possibility that our seasonal adjustment process of the raw data is not driving or results. As the year on year inflation rate compares the price level of the month of interest with the same month from last year, there should not be any seasonal patterns visible. Fortunately, the results remain robust qualitatively as well as quantitatively. Thus, the seasonal adjustment process seems to be appropriate.

Appendix 3: Data Sources

Table 9: Variables definition and data sources. All data is taken for Germany. The table reports all the data we use in the different model specifications and robustness checks.

Variables	Source	Sample
2m temperature (ERA5 Land)	CDS	1970m1-2021m12
Population (regional)	INKAR	1996-2021
Agricultural Area (regional)	INKAR	2016-2021
HICP - Overall index	Eurostat	1996m1-2021m12
HICP - Energy	Eurostat	1996m1-2021m12
HICP - Food (incl. alcohol and tobacco)	Eurostat	1996m1-2021m12
HICP - Processed food (incl. alcohol and tobacco)	Eurostat	1996m1-2021m12
HICP - Unprocessed food	Eurostat	1996m1-2021m12
HICP - Excl. energy, food, alcohol and tobacco	Eurostat	1996m1-2021m12
HICP - Services (excl. goods)	Eurostat	1996m1-2021m12
Production in Industry (total)	Eurostat	1996m1-2021m12
Call Money/Interbank Rate: Total for Germany	FRED	1996m1-2021m12
Euro area shadow rate	Wu and Xia (2017)	2004m9-2021m12
Power generation and consumption	Agorameter	2012m1-2021m12
Sun Duration	DWD	1996m1-2021m12
Precipitation	DWD	1996m1-2021m12
Growing Season (start- & end date)	World Bank	1996-2021

Figure 14: Impulse response functions for different components of the harmonized index of consumer prices, shown for temperature anomalies during each calendar season. The respective shaded areas represent 68% confidence intervals computed using Newey–West standard errors.

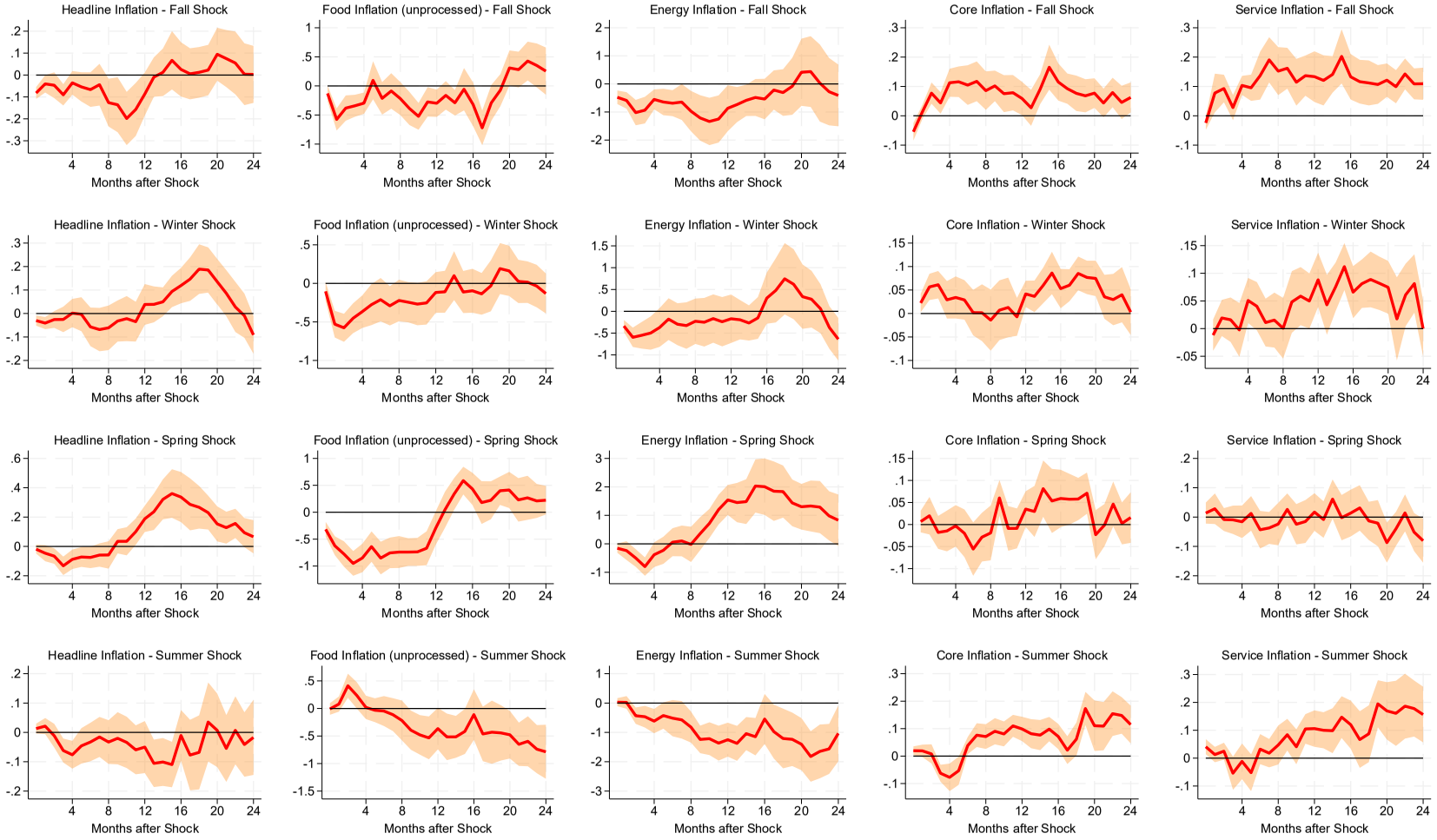

Figure 15: Impulse response functions for different components of the harmonized index of consumer prices, shown for hot and cold temperatures separately. Local shocks were aggregated using GDP weights. The respective shaded areas represent 68% confidence intervals computed using Newey–West standard errors.

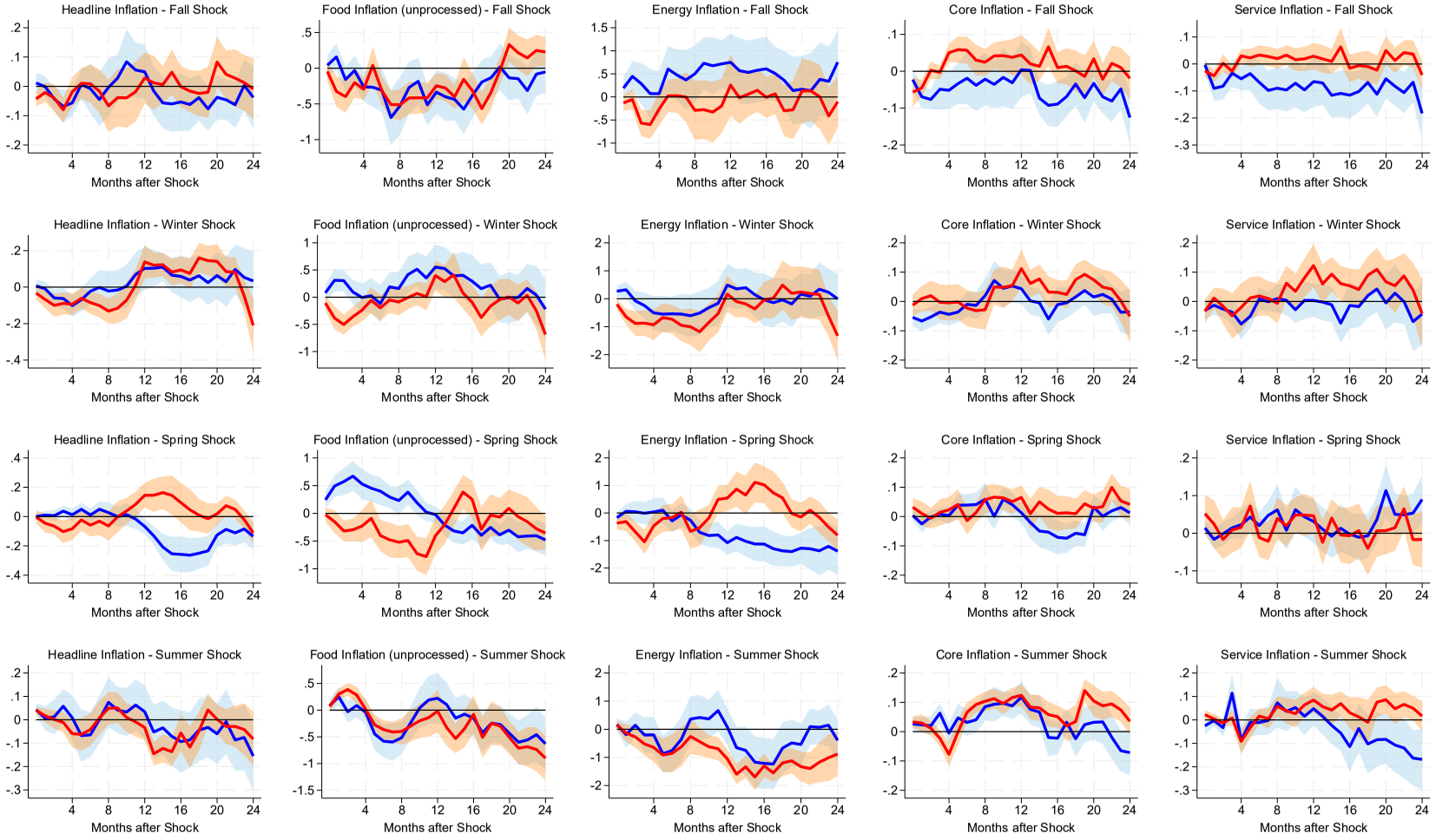

Figure 16: Impulse response functions for different components of the harmonized index of consumer prices, shown for hot and cold temperatures separately. Local shocks were aggregated using agricultural area weights. The respective shaded areas represent 68% confidence intervals computed using Newey–West standard errors.

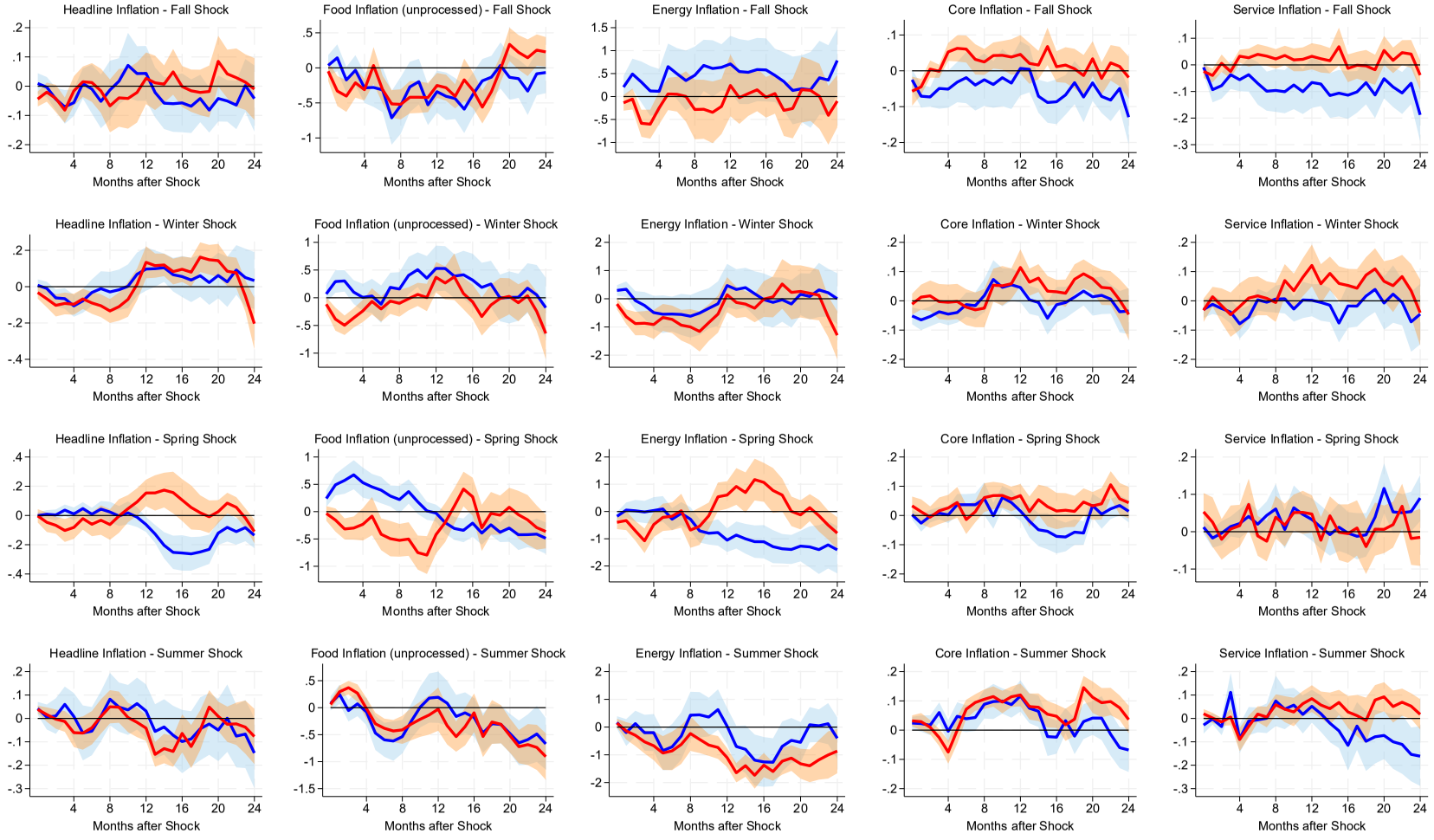

Figure 17: Impulse response functions for different components of the harmonized index of consumer prices, shown for hot and cold temperatures separately. Learning period of 2 years. The respective shaded areas represent 68% confidence intervals computed using Newey–West standard errors.

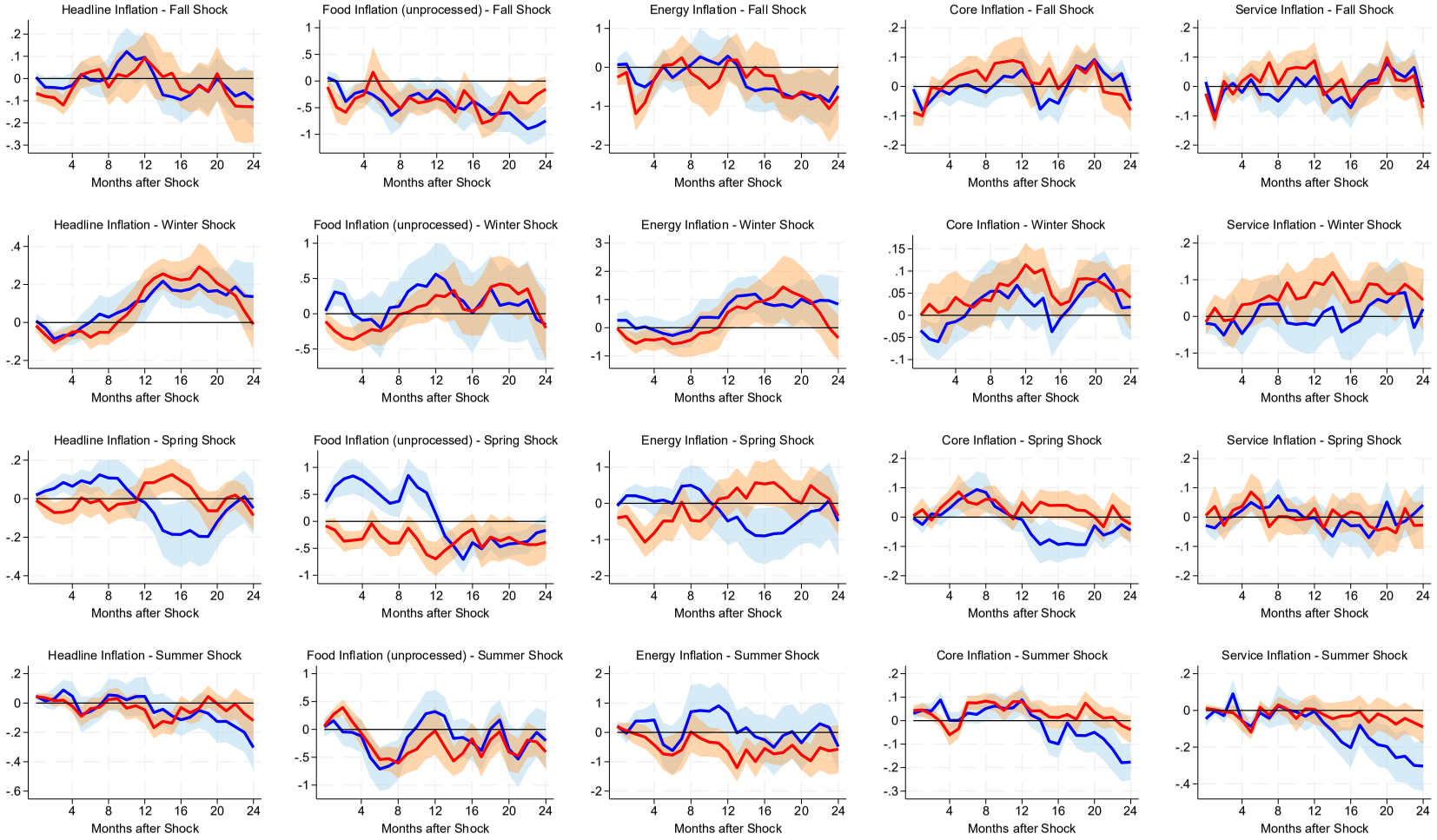

Figure 18: Impulse response functions for different components of the harmonized index of consumer prices, shown for hot and cold temperatures separately. Learning period of 10 years. The respective shaded areas represent 68% confidence intervals computed using Newey–West standard errors.

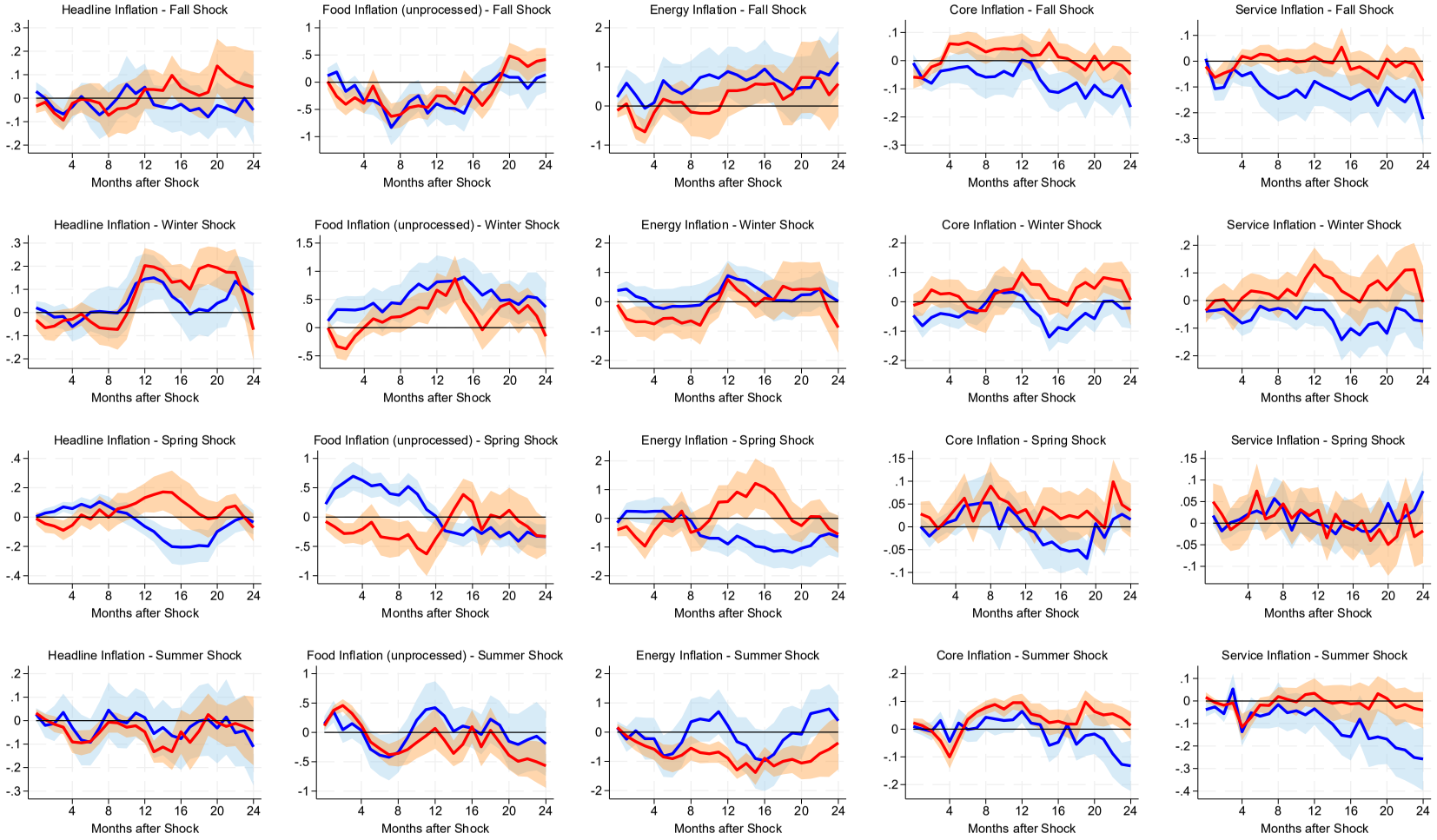

Figure 19: Impulse response functions for different components of the harmonized index of consumer prices, shown for hot and cold temperatures separately. The dependent variable is the year-on-year inflation rate for the respective component. The respective shaded areas represent 68% confidence intervals computed using Newey–West standard errors.